

Beyond the MSSM Higgs bosons at the 7 TeV LHCMarcela Carena,^{1,2,3} Eduardo Pontón,⁴ and José Zurita⁵¹*Theoretical Physics Department, Fermilab, Batavia, Illinois 60510, USA*²*Enrico Fermi Institute, Chicago, Illinois 60637, USA*³*Kavli Institute for Cosmological Physics, The University of Chicago, Chicago, Illinois 60637, USA*⁴*Department of Physics, Columbia University, 538 W. 120th St, New York, New York 10027, USA*⁵*Institut für Theoretische Physik, Universität Zürich, Winterthurerstrasse 190, CH-8057 Zürich, Switzerland*

(Received 20 November 2011; published 8 February 2012)

We consider the Higgs sector in extensions of the minimal supersymmetric standard model by higher-dimension operators in the superpotential and the Kähler potential, in the context of Higgs searches at the LHC 7 TeV run. Such an effective field theory approach, also referred to as BMSSM, allows for a model-independent description that may correspond to the combined effects of additional supersymmetric sectors, such as heavy singlets, triplets or gauge bosons, in which the supersymmetry-breaking mass splittings can be treated as a perturbation. We consider the current LHC dataset, based on about $1\text{--}2\text{ fb}^{-1}$ of data to set exclusion limits on a large class of BMSSM models. We also present projections for integrated luminosities of 5 and 15 fb^{-1} , assuming that the ATLAS and CMS collaborations will combine their results in each channel. Our study shows that the majority of the parameter space will be probed at the 2σ level with 15 fb^{-1} of data. A nonobservation of a Higgs boson with about 10 fb^{-1} of data will point towards a Higgs SUSY spectrum with intermediate $\tan\beta$ (\approx a few to 10) and a light SM-like Higgs with somewhat enhanced couplings to bottom and tau pairs. We define a number of BMSSM benchmark scenarios and analyze the possible exclusion/discovery channels and the projected required luminosity to probe them. We also discuss the results of the effective field theory framework for two specific models, one with a singlet superfield and one with $SU(2)_L$ triplets.

DOI: [10.1103/PhysRevD.85.035007](https://doi.org/10.1103/PhysRevD.85.035007)

PACS numbers: 12.60.Jv, 14.80.Da

I. INTRODUCTION

The search for a standard model (SM) Higgs boson responsible for electroweak symmetry breaking has been the central focus of both the Tevatron and the LHC in the recent past, and it remains one of the main goals for the LHC in the years to come. Present LEP, Tevatron and LHC data have already placed strong direct bounds on the possible mass of such a Higgs particle, leaving an allowed range between 114 GeV and 145 GeV, and above ~ 450 GeV [1,2].

Several shortcomings of the SM model (the Planck/weak scale hierarchy, the origin of fermion masses and mixing angles, dark matter and baryogenesis) could be addressed by beyond-the-SM extensions at or somewhat above the TeV scale. Some of these advocate a perturbative extension as in supersymmetric theories, whereas others involve strong dynamics as in extended technicolor/topcolor/topcondensate theories or theories with extra dimensions. All these possible extensions address the question of electroweak symmetry breaking via different mechanisms that may imply the presence of various extended Higgs sectors, in which the Higgs couplings to the known particles can vary significantly (or there may be no Higgs at all). It is of major importance to explore different theoretical SM extensions that can alter the expected SM Higgs production and decay modes, thereby allowing for very different interpretations of the experimental Higgs mass bounds.

In the past years there has been extensive work in extensions of the Higgs sector of the minimal supersymmetric standard model (MSSM) by higher-dimension operators [3]. Indeed, several different aspects related to fine-tuning, the Higgs potential, dark matter, electroweak baryogenesis, flavor physics, and CP -violation have been studied considering the effects of higher-dimension operators of dimension-five in the superpotential [4] and dimension-six in the Kähler potential [5–7].

In this article we will consider the effective field theory (EFT) approach described in Ref. [6] and study the effects of such a beyond-the-MSSM (BMSSM) theory on Higgs searches at the LHC. The EFT framework allows for a model-independent description of a large class of extensions of the MSSM, which may include the combined effects of many additional sectors at energies somewhat above the electroweak scale, that can impact the Higgs phenomenology. It provides an opportunity to use the Higgs sector as a window on BMSSM physics. On the other hand, this EFT approach can also be reinterpreted to explore the Higgs LHC potential for some specific MSSM extensions, such as the addition of heavy singlets, triplets or gauge bosons. In particular, we will show that our approach can reproduce to a good level of accuracy results of simple renormalizable supersymmetric (SUSY) models. One should note, however, that the study of the EFT in superfield language relies on the assumption that the UV theory at a scale M is supersymmetric up to small

supersymmetry-breaking effects of order m_s (m_s being of order the electroweak scale), that can be treated as a perturbation.

The phenomenology of the BMSSM Higgs sector up to dimension-six operators in the superpotential and Kähler potential, including all possible SUSY-breaking effects via spurion superfields, was studied in detail in Ref. [6]. At leading order in $1/M$, the superpotential reads

$$W = \mu H_u H_d + \frac{\omega_1}{2M} [1 + \alpha_1 X] (H_u H_d)^2, \quad (1)$$

where $H_u H_d = H_u^0 H_d^0 - H_u^+ H_d^-$, and ω_1 and α_1 are dimensionless parameters that we assume to be of order one. The second term in the square brackets is the soft supersymmetry-breaking term parametrized via a (dimensionless) spurion superfield $X = m_s \theta^2$. At order $1/M^2$ there are no operators in the superpotential, but several operators enter through the Kähler potential:

$$K = H_d^\dagger e^{2V} H_d + H_u^\dagger e^{2V} H_u + \Delta K^{\text{SUSY}} + \Delta K^{\delta\text{SUSY}}, \quad (2)$$

where

$$\begin{aligned} \Delta K^{\delta\text{SUSY}} = & \frac{c_1}{2|M|^2} (H_d^\dagger e^{2V} H_d)^2 + \frac{c_2}{2|M|^2} (H_u^\dagger e^{2V} H_u)^2 \\ & + \frac{c_3}{|M|^2} (H_u^\dagger e^{2V} H_u) (H_d^\dagger e^{2V} H_d) \\ & + \frac{c_4}{|M|^2} |H_u H_d|^2 + \left[\frac{c_6}{|M|^2} H_d^\dagger e^{2V} H_d \right. \\ & \left. + \frac{c_7}{|M|^2} H_u^\dagger e^{2V} H_u \right] (H_u H_d) + \text{H.c.}, \quad (3) \end{aligned}$$

and ΔK^{SUSY} contains all the SUSY-breaking operators associated with the operators of Eq. (3) by multiplication by X , X^\dagger or $X^\dagger X$. We assume that the coefficients of these SUSY-breaking operators are proportional to the corresponding c_i , with proportionality constants of order one, that we call β_i , γ_i and δ_i (see Ref. [6] for the detailed definitions).

It was shown that the inclusion of the above higher-dimension operators alleviates the tension present in the MSSM between the upper theoretical bound of about 135 GeV and the nonobservation at LEP of a Higgs boson, as well as allowing for a Higgs phenomenology markedly different from the MSSM. In Ref. [7] we interpreted the LEP and Tevatron Higgs boson bounds in the light of a parameter scan of BMSSM models and defined a number of benchmark scenarios with interesting Higgs phenomenology. In this paper we study constraints and prospects for detectability of extensions of the MSSM at the LHC Run-I and we also present the results in specific models such as the MSSM with an extra heavy singlet and the MSSM with extra heavy triplets. We base our results on the current data from Higgs searches at the LHC at a center of mass energy of 7 TeV, with about $1\text{--}2 \text{ fb}^{-1}$ of integrated luminosity per experiment (depending on the channel) [8–20], and extrapolate the expected results for two scenarios: 5 and 15 fb^{-1} of integrated luminosity.

The most sensitive channels to search for a SM Higgs boson at the LHC are highly dependent on its mass. If the Higgs is light, in the 115–120 GeV range, the most sensitive channel is the diphoton ($\gamma\gamma$) one. For intermediate masses (120–205 GeV) it is the WW channel, and for heavier bosons (205–600 GeV), the ZZ channel. When considering neutral Higgs bosons of an extended sector (like in supersymmetric theories), generically denoted by Φ , this situation can change according to how these Higgs bosons couple to the SM particles. Nevertheless, we expect at least one of them to couple sizably to the W and Z gauge bosons, and therefore these decay modes may also be useful to probe neutral Higgs bosons from such nonminimal sectors. Similarly, sizable couplings to the top quark can induce important couplings to photons at loop level, just like for the SM Higgs. In addition, Higgs decays into down-type fermions, such as $V\Phi$, $\Phi \rightarrow b\bar{b}$, $q\bar{q}\Phi$, $\Phi \rightarrow \tau^+\tau^-$, or the inclusive decay into $\tau^+\tau^-$ can also be useful to probe a neutral Higgs boson. In the SM, the latter channel does not constitute an early discovery mode. However, if one has an enhanced coupling to bottom pairs that enhances the production cross section, as in the large $\tan\beta$ regime of the MSSM, it can turn into a discovery mode (see Ref. [21] for a recent study of the LHC Run-I reach within the MSSM).

We are particularly interested in the first few to ten inverse femtobarns of LHC data, where many of these channels will start to show sensitivity to the Higgs boson. Other implications of early LHC results have been recently considered in the context of SUSY singlet extensions [22], in more general two-higgs doublet model scenarios [23], and also for dark Higgs models [24] (where the SM Higgs sector is enlarged with a SM singlet). With the current dataset, Tevatron bounds coming from the WW decay mode [25,26] are already superseded by the LHC [8–10]. With a few inverse femtobarn of data, the diphoton channel will be able to probe points where the cross section times branching fraction is close to the SM one [27,28], which may be compared to the current Tevatron factor of about 15 [29,30]. In the low mass region, $V\Phi$, $\Phi \rightarrow b\bar{b}$ rates close to the SM one can be explored at the Tevatron, whereas they require a larger dataset at the LHC. The ZZ channel [28] will also be effective to rule out Higgs bosons with a mass in the 200–600 GeV range. Such a mass range cannot be probed at the Tevatron since the corresponding production cross sections are very small.

This paper is organized as follows. In Sec. II, we summarize the most relevant Higgs search channels at the LHC Run-I. In Sec. III we present our results, showing the reach of LHC Run-I for different BMSSM scenarios and specific decay channels. We also update the prospects for the benchmark points presented in Ref. [7], separating the analysis into the low and large $\tan\beta$ regimes. In Sec. IV we study MSSM extensions with a heavy singlet and with heavy triplets using the EFT approach. We conclude in Sec. V.

II. PROBING THE HIGGS SECTOR WITH EARLY LHC DATA

In this section we present all the Higgs search channels at the LHC that will be used in our study. We will employ data when available in order to take into account the most up-to-date experimental details (e.g., efficiencies, acceptances and background estimations) from the LHC collaborations. However, for $V\Phi$, $\Phi \rightarrow b\bar{b}$ and $qq\Phi$, $\Phi \rightarrow \tau^+\tau^-$ we employ the available MC simulations.¹ Throughout this work we will consider the following Higgs search channels:

- (a) $pp \rightarrow \Phi \rightarrow WW, ZZ, \gamma\gamma$,
- (b) $pp \rightarrow \Phi \rightarrow \tau^+\tau^-$,
- (c) $V\Phi$, $\Phi \rightarrow b\bar{b}$, and $qq\Phi$, $\Phi \rightarrow \tau^+\tau^-$,
- (d) $t \rightarrow H^+b$.

The channels listed in a) and c) are conventional SM Higgs search channels at the LHC, the only difference being that c) are not expected to be discovery modes for a SM Higgs boson in LHC Run-I. The inclusive tau channel, b), has a very low rate in the SM, but can be enhanced in nonminimal scenarios. This situation arises when one neutral Higgs boson couples very weakly to gauge bosons and has enhanced couplings to down-type fermions, as in the large $\tan\beta$ limit of the MSSM, or in the decoupling limit, where $m_A \sim m_H \gg m_h$ and H is gaugephobic. Finally, a charged Higgs lighter than the top quark can also be looked for in channel d), and can be interesting at the LHC with a relatively small dataset.

We will summarize first the ‘‘SM-like Higgs searches,’’ focusing on the channels a), but also including channels c). Later, in Sec. II B, we will analyze separately the inclusive tau case, b). Finally, we will discuss the reach for a charged Higgs boson in Sec. II C.

A. SM-like Higgs Searches

In our analysis we consider all present direct experimental bounds on a SM Higgs and reinterpret them in terms of our BMSSM scenarios. We take into account all the bounds from LEP and Tevatron searches via HIGGSBOUNDS v2.1.1 [31,32], and focus on those models that are *not excluded* by these experiments at the 95% confidence level (CL). For the LHC analysis, we consider the most recent data of the ATLAS and CMS collaborations in the WW [8–10], ZZ [11–14] and $\gamma\gamma$ [15,16] channels, based on 1.04–2.28 fb^{-1} of integrated luminosity. These channels are the most sensitive ones to a SM Higgs boson, in the mass ranges given earlier. For the associated production with a weak gauge boson (Higgs-strahlung), with the Higgs decaying into $b\bar{b}$, both ATLAS [33] and CMS [19] have recently presented results with about 1 fb^{-1} of data. The current

¹These channels do not yet play a major role, but we have included them for completeness.

TABLE I. List of LHC channels used in this study, indicating the luminosity used by the collaborations in the analysis. The ‘‘...’’ indicates that no data for that particular channel has been presented by the corresponding collaboration. Here, Φ stands for any neutral Higgs boson. The production mechanisms considered are gluon fusion, vector-boson fusion, associated production with $Z, W, t\bar{t}$ and also $b\bar{b} \rightarrow \Phi$ (only relevant for large $\tan\beta$).

Channel	Lum. (fb^{-1})		Mass range (GeV)	Ref.
	ATLAS	CMS		
$pp \rightarrow \Phi \rightarrow WW$	1.7	1.55	115–600	[8–10]
$pp \rightarrow \Phi \rightarrow ZZ$	1.04–2.28	1.1–1.7	120–600	[11–14]
$pp \rightarrow \Phi \rightarrow \gamma\gamma$	1.08	1.7	110–150	[15,16]
$pp \rightarrow \Phi \rightarrow \tau^+\tau^-$	1.06	1.6	90–600	[17,18]
$V\Phi, \Phi \rightarrow b\bar{b}$...	1.1	110–135	[19]
$qq\Phi, \Phi \rightarrow \tau^+\tau^-$	1	...	110–130	[28]
$t \rightarrow H^+b, H^+ \rightarrow \tau^+\nu_\tau$...	1.1	80–160	[20]

CMS search is sensitive to a rate of about 6 times the SM one, while the ATLAS search can only exclude a rate of about 20 times the SM. Note, however, that in the Monte Carlo 2010 ATLAS sample [28], where the boosted $b\bar{b}$ pair techniques of [34] were employed, the expected sensitivity with 1 fb^{-1} was very similar to the recent CMS result. For the $qq\Phi$, $\Phi \rightarrow \tau^+\tau^-$ channel, for which no LHC collaboration has presented data, we employ the MC2010 sample. Finally, we add the LHC searches for $\Phi \rightarrow \tau^+\tau^-$, which are discussed in detail in Sec. II B.

In the channels where both CMS and ATLAS have presented data, we combine their results following the simple prescription described in Refs. [35,36]. Although this procedure may be overly simplistic, and a careful combination by the experimental collaborations would be most welcome, it allows us to get an idea of the present exclusion bounds with the information available. Therefore, when applied to our scan over BMSSM scenarios, our *current exclusion* statements will refer to such a combination of the observed limits by both experiment. For channels where only one collaboration has presented an analysis, we will base our current exclusion on that analysis. The *projections* of the LHC reach for a given luminosity, on the other hand, are computed using the method described in Appendix B. For channels where only one collaboration has presented data, we assume that the expected limit of the other collaboration will be similar, and ‘‘double’’ the expected projected dataset (we call it $\text{CMS} \times 2$ or $\text{ATLAS} \times 2$).² Thus, our *projections* should always be interpreted as what would be expected from a combination of both experiments. A summary of the various datasets used in this work is presented in Table I.

²Given that, as explained above, the expected ATLAS sensitivity in the $V\Phi$, $\Phi \rightarrow b\bar{b}$ channel after improving their analysis should be similar to the expected CMS exclusion limit, we employ the $\text{CMS} \times 2$ prescription for the projections in this channel.

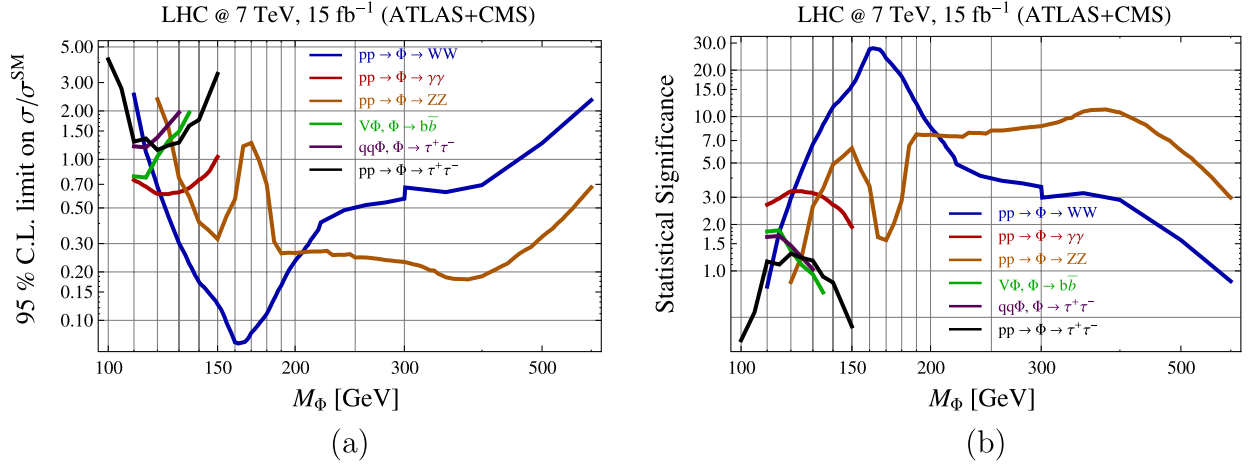


FIG. 1 (color online). LHC reach (a) and significances (b) for the SM Higgs boson with 15 fb⁻¹, combining both experiments. The color coding is as follows: WW (blue), ZZ (orange), $\gamma\gamma$ (red), $\tau^+\tau^-$ (black), $V\Phi$, $\Phi \rightarrow b\bar{b}$ (green), $qq\Phi$, $\Phi \rightarrow \tau^+\tau^-$ (purple) and $\tau^+\tau^-$ inclusive (black). Figure taken from Ref. [24].

We present in Fig. 1 (taken from Ref. [24]) the expected 95% C L exclusion limit on Higgs production cross sections (including the corresponding decay rates) normalized to their SM values as a function of the Higgs mass for a total integrated luminosity of 15 fb⁻¹. We also show the statistical significance of the different channels as a function of the Higgs mass for the same integrated luminosity. We see that the WW channel has exclusion power down to $M_\Phi \sim 115$ GeV and up to $M_\Phi \sim 450$ GeV. It is actually the most sensitive channel for $120 \text{ GeV} \leq M_\Phi \leq 205$ GeV, while for larger masses the ZZ signal takes over this role. For masses in the 115–150 GeV range, one can test signals in the diphoton channel as low as 0.6–0.7 times the SM rate (2σ exclusion), and test the SM up to about 3σ . The remaining channels are less powerful in probing the SM Higgs at the LHC Run-I.

B. Non-SM neutral Higgs searches in the $\tau^+\tau^-$ channel

This search is important for neutral Higgs bosons in the MSSM at large values of $\tan\beta$, where the bottom Yukawa coupling is enhanced, thus yielding a significant increase in the rate. The current analyses of ATLAS [17] (1.06 fb⁻¹) and CMS [18] (1.6 fb⁻¹), taken individually, are able to probe a rate of about 10 times the SM one, for masses between 110–150 GeV, already 1 order of magnitude better than the current results from Tevatron (combining CDF and D0) [37].

In this study, we are interested in the bounds on the $h/H/A \rightarrow \tau^+\tau^-$ cross sections presented by the LHC collaborations, which extend up to Higgs masses of about 600 GeV. ATLAS [17] reports individual 95% CL limits for the $gg \rightarrow \Phi$ and $b\bar{b}\Phi$ production modes ($\Phi = h, H, A$), while CMS [18] presents a combined result of these two production channels. In order to obtain the exclusion limit, we compute in each of our model points the $gg \rightarrow \Phi \rightarrow$

$\tau^+\tau^-$ and $bb\Phi$, $\Phi \rightarrow \tau^+\tau^-$ rates, and derive the Q values, as defined in Appendix B [see Eq. (B1)], one for each of the three experimental limits above. The production cross sections and branching fractions at the LHC are taken from Ref. [38], except for the $bb\Phi$ cross section, that was obtained using the code BBH@NNLO [39] with the MSTW 2008 PDF set [40]. If the masses of two or more Higgs bosons fall within 10 GeV of each other we add the corresponding signals. We then combine the three significances (from ATLAS in $gg \rightarrow \Phi$, ATLAS in $bb\Phi$ and CMS combined) in quadrature to obtain a total significance in the $\tau^+\tau^-$ channel for each scenario of our BMSSM parameter scan.

C. Charged Higgs searches in top decays

Besides the neutral Higgs sector, one can also probe at the LHC a charged Higgs boson, produced in the decay of the top quark. This decay mode is effective only for $m_{H^+} < m_t - m_b$. The tree-level partial decay widths for $t \rightarrow W^+b$ and $t \rightarrow H^+b$ are given by [41]

$$\Gamma(t \rightarrow W^+b) = \frac{G_F}{8\pi\sqrt{2}} m_t^3 \lambda^{1/2}(1, x_b, x_w) \times [x_w(1 + x_b) + (1 - x_b)^2 - 2x_w^2], \quad (4)$$

and

$$\Gamma(t \rightarrow H^+b) = \frac{G_F}{8\pi\sqrt{2}} m_t^3 \lambda^{1/2}(1, x_b, x_{H^+}) \times \left[\left(\frac{1}{\tan\beta^2} + x_b \tan\beta^2 \right) (1 + x_b - x_{H^+}) + 4x_b \right], \quad (5)$$

where $\lambda(a, b, c) = a^2 + b^2 + c^2 - 2ab - 2ac - 2bc$ and $x_i = m_i^2/m_t^2$. We also implement the NLO QCD corrections to both $t \rightarrow W^+b$ [42] and $t \rightarrow H^+b$ [43,44]. For the

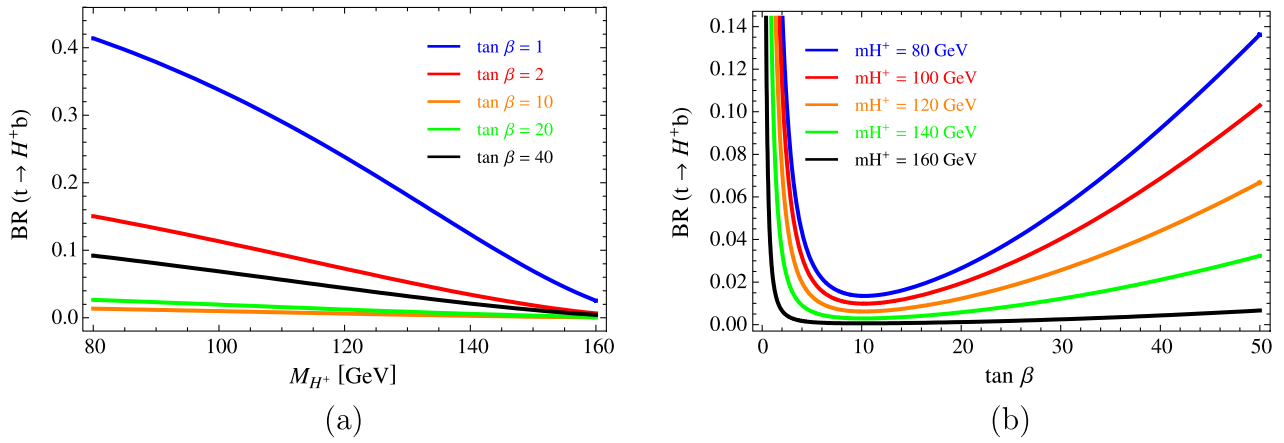


FIG. 2 (color online). Branching fraction of the top quark into a charged Higgs and a bottom quark as a function of (a) m_{H^+} and (b) $\tan\beta$. SUSY QCD corrections are not included.

W -channel we use a QCD K-factor $K = 1 - (2\alpha_s/3\pi) \times (2\pi^2/3 - 5/2) \approx 0.91$ [42], where $\alpha_s \approx 0.107$ is evaluated at $\mu = m_t$. For the Higgs channel we implement the results of [44], which hold for any value of $\tan\beta$. At small $\tan\beta$ these QCD corrections are small (below 10%), but they can be sizable at larger $\tan\beta$. Also, at large $\tan\beta$ the SUSY QCD corrections can be important. To take these latter effects into account we use the SUSY QCD corrections presented in [45], which amount to using an effective bottom Yukawa coupling corrected by $1/(1 + \Delta_b)$, where Δ_b depends on the SUSY spectrum [46].

As a guide, in Fig. 2 we show the branching fraction of the top quark decaying into a charged Higgs plus a bottom quark, as a function of the charged Higgs mass (left panel) and also as a function of $\tan\beta$, including only the QCD corrections of [44]. However, when applied to our scan over BMSSM scenarios, and for the $\tan\beta > 10$ cases, we will also include the SUSY QCD corrections described above (assuming gluinos and squarks at 1 TeV, negligible A -terms and $\mu > 0$).³ For the values of $\tan\beta$ that will be employed in this work (2 and 20), we see that this branching ratio is always below 20%, and decreases with increasing m_{H^+} , due to a phase space suppression. From the right panel we see that there is a minimum around $\tan\beta \sim \sqrt{m_t/m_b} \sim 8$, where m_b is evaluated at the scale of the top mass. For a fixed charged Higgs mass, the branching fraction grows for either very large or small values of $\tan\beta$.

To set limits and make projections, we use the latest CMS search [20] for a charged Higgs produced in top decays, which assumes that $\text{BR}(H^+ \rightarrow \tau^+ \nu_\tau) = 1$. We will therefore apply this limit only to models where $\text{BR}(H^+ \rightarrow \tau^+ \nu_\tau) > 0.9$, and in those cases we will interpret the CMS bound as applying to $\text{BR}(t \rightarrow H^+ b) \times \text{BR}(H^+ \rightarrow \tau \nu)$. We expect that this procedure will give a

³For $\mu < 0$ the corrections due Δ_b can significantly enhance the branching fraction into the charged Higgs channel [45].

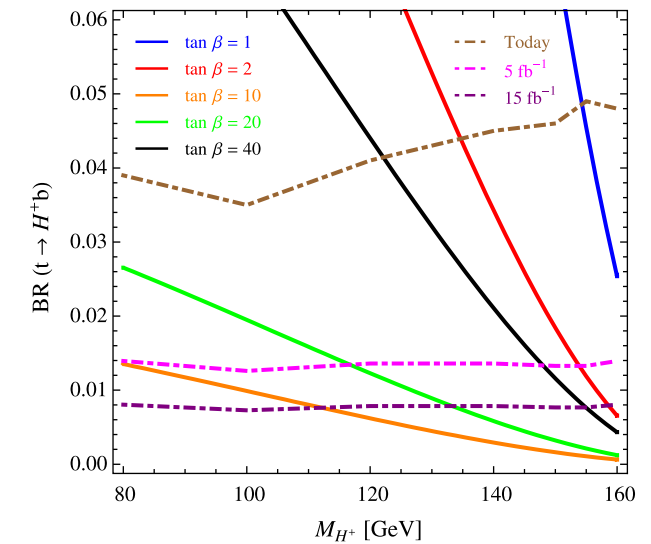


FIG. 3 (color online). The current CMS 95% CL upper bound on $\text{BR}(t \rightarrow H^+ b)$ (dot-dashed brown) [20], together with the projected (CMS $\times 2$) LHC reach for 5 and 15 fb^{-1} , shown in dot-dashed purple and pink curves. The region above the dot-dashed curves would be excluded at the specified total integrated luminosity. The solid lines correspond to $\tan\beta = 1$ (blue), 2 (red), 10 (orange), 20 (green) and 40 (black). SUSY QCD corrections are not included.

good estimate of the LHC charged Higgs reach for BMSSM scenarios with such a dominant $\tau\nu$ decay channel.⁴ In Fig. 3, the dot-dashed brown curve corresponds to the CMS observed limit on $\text{BR}(t \rightarrow H^+ b)$. We also show curves of $\text{BR}(t \rightarrow H^+ b)$ as a function of m_{H^+} for fixed

⁴We also ignore the modified $H^+ b t$ coupling due to the canonical renormalization required when introducing dimension-six operators (see Ref. [6]). This is a small effect, always below 4 (3) % for $\tan\beta = 2$ (20), and thus will be neglected throughout this paper.

$\tan\beta$, using Eqs. (4) and (5), with the QCD corrections of [44] taken into account.

We see from these figures that for $\tan\beta = 2$ the charged Higgs is very constrained: one can exclude values below about 135 (160) GeV with 1(15) fb^{-1} , where for the projection we use the “CMS $\times 2$ ” prescription. For $\tan\beta = 20$, where the NLO QCD corrections are larger, there is currently no exclusion for $m_{H^\pm} > 80$ GeV. With 5(15) fb^{-1} one will start to probe masses up to about 120 (135) GeV. However, we note that the inclusion of the SUSY QCD corrections for the supersymmetric parameters considered in this work weakens the 7 TeV LHC run reach, and can only probe charged Higgs masses up to 105 (125) GeV for total integrated luminosities of 5(15) fb^{-1} . On the other hand, for other choices of the supersymmetric parameters (e.g., with $\mu < 0$), larger charged Higgs masses could be probed for such luminosities.

III. RESULTS

In this section we present the results of our analysis for BMSSM scenarios. We use the same sample of points that was used in Ref. [6,7], to which we added a sparse scan over $\tan\beta$ (see Ref. [6] for technical details on how the scan was performed). In brief, these points are consistent with electroweak precision data and do not receive sizable corrections from higher-dimension operators (namely, the perturbative series in powers of $1/M$ seems to converge). Moreover, our working assumption is that there exist BMSSM degrees of freedom with masses of about 1 TeV that couple with order-one couplings to the MSSM Higgs sector. Thus, these scenarios always represent significant departures from the MSSM and our conclusions regarding exclusion or discovery prospects cannot be simply applied to the MSSM limit. We have considered stops of about 300 GeV to emphasize that radiative corrections play a minor role in the Higgs spectrum, but they could be somewhat heavier without significantly changing our results.⁵ For the majority of our analysis we explore two values for $\tan\beta$: 2 and 20, which are taken to be representative of the small and large $\tan\beta$ regimes. At even larger values of $\tan\beta$, the effects of the BMSSM sector are smaller. We also consider a smaller parameter scan for intermediate values of $\tan\beta$ between 4 and 8, which turns to be more challenging for the ongoing LHC run.

⁵A recent ATLAS study shows some sensitivity to a lightest stop with mass $m_{\tilde{t}_1} \sim 300$ GeV provided the gluino mass is around 500 GeV [47]. Similarly, sbottoms can be bounded by about 600 GeV provided the gluino mass is below 750 GeV [48], and by about 250 GeV for neutralino masses below 110 GeV [49]. However, for heavier gluinos or neutralinos the bounds on the stop/sbottom masses essentially disappear. Furthermore, gluinos and first two-generation squarks may have to be heavier than about 1 TeV [50]. These latter particles play no relevant role in our study.

We will present the current and projected LHC Run-I constraints on our sample, and update the benchmark scenarios presented in Ref. [7]. As we will see some of these scenarios have been excluded by the latest LHC studies. We will also present further benchmark points that illustrate the exclusion/discovery prospects at the 7 TeV LHC run.

A. Global constraints from the LHC

In this subsection we present plots that illustrate some generic features of BMSSM scenarios in connection to LHC Higgs phenomenology. In Fig. 4 we show our scan of points, in the $m_H - m_h$ plane, for $\tan\beta = 2$. In the left panel we plot all the points currently *not excluded* by LEP or Tevatron data. We show in green those points that are excluded by the most recent LHC limits (combining data from both collaborations), while those that require a total integrated luminosity of 5 and 15 fb^{-1} to be within reach of the LHC, are shown in magenta and blue, respectively. Points outside of LHC Run-I reach are shown in red. The dotted line shows the MSSM result, which we provide as a reference (for such light stops, the MSSM would be excluded by LEP). The LEP constraints rule out points with low values of m_h . The few allowed points with $m_h \lesssim 100$ GeV are not probed by LEP due to a very reduced coupling of the lightest CP -even Higgs to gauge bosons (H is SM-like), which suppresses the Higgs-strahlung production cross section. Tevatron bounds explain the absence of points with m_h in the 160–180 GeV range, the exceptions corresponding to cases where the coupling of h to WW and ZZ is sufficiently smaller than their SM counterpart. The current LHC limits extends this range to 135–250 GeV. With 15 fb^{-1} , one will further probe points down to 115 GeV, either in the $h \rightarrow WW$ or $h \rightarrow \gamma\gamma$ channel, thus excluding most of the scanned points. The cases that cannot be tested at the 2σ level with 15 fb^{-1} correspond to points where the CP -odd Higgs A is light and therefore one or both CP -even Higgs bosons have a sizable branching ratio into AA , or points where the branching ratio into $b\bar{b}$ is enhanced compared to the SM, thus reducing the WW and $\gamma\gamma$ branching fractions.

In the right panel of Fig. 4 we plot those points which are within the *discovery* reach of the LHC with 15 fb^{-1} of total integrated luminosity, combining both experiments. Besides the currently allowed points (significance less than 2σ), we also include in this plot those points that are currently excluded at a significance between 2σ and 3σ , to account for a possible downward fluctuation in current data. For this subset (i.e., “exclusion significance below 3σ ”), we indicate by the color code the most sensitive channel to discover a Higgs boson: $pp \rightarrow h \rightarrow WW$ (green), $pp \rightarrow H \rightarrow WW$ (magenta), $pp \rightarrow h \rightarrow ZZ$ (blue), $pp \rightarrow H \rightarrow ZZ$ (red), $pp \rightarrow h \rightarrow \gamma\gamma$ (brown), and $t \rightarrow H^+ b$ (orange).

In Fig. 5 we show the same information as in Fig. 4, but for $\tan\beta = 20$. One sees in the left panel that the

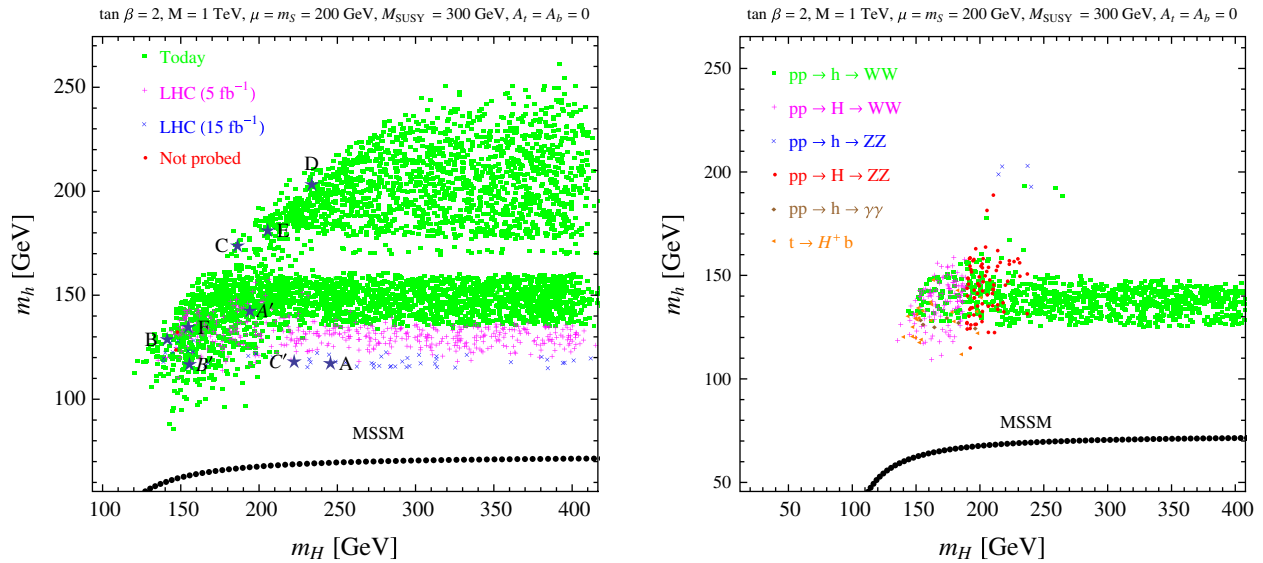


FIG. 4 (color online). Scan over BMSSM scenarios, for $\tan\beta = 2$. Upper: Points not excluded by LEP or Tevatron data at the 95% CL. We show points currently excluded by the LHC with 1 fb^{-1} in green. The LHC exclusion reach for 5 and 15 fb^{-1} is shown in magenta and blue, while points outside the LHC Run-I reach are plotted in red. Lower: Models that can be discovered (5σ) after 15 fb^{-1} of collected data, assuming an ATLAS/CMS combination in each separate channel. We include here those points that are currently excluded at less than 3σ (most currently excluded points are excluded at more than 3σ). We indicate the discovery mode: $pp \rightarrow h \rightarrow WW$ (green), $pp \rightarrow H \rightarrow WW$ (magenta), $pp \rightarrow h \rightarrow ZZ$ (blue), $pp \rightarrow H \rightarrow ZZ$ (red), $pp \rightarrow h \rightarrow \gamma\gamma$ (brown) and $t \rightarrow H^+ b$ (orange). Note that the color code is different in the two plots.

current bounds make sharp cuts on the parameter space: LEP rules out points with $m_h \lesssim 114.4 \text{ GeV}$, while the Tevatron excludes the heavy mass points, effectively setting an upper bound on our sample of around 160 GeV . The 7 TeV run of the LHC can exclude all of our scanned points with a significance larger than 2σ

for a total integrated luminosity of about 16 fb^{-1} . It is worth stressing that for $\tan\beta = 20$ there is a significant number of models being probed by the $\tau^+ \tau^-$ decay mode (about half of the points tested at less than 3σ with the ATLAS and CMS analyses of the summer of 2011).

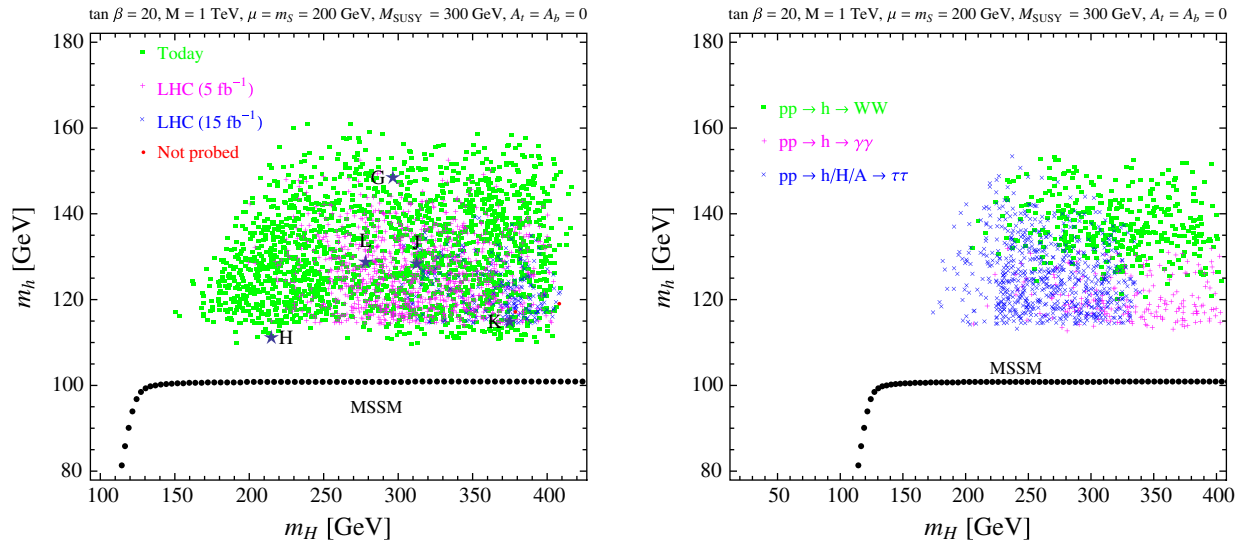


FIG. 5 (color online). Scan over BMSSM scenarios, for $\tan\beta = 20$. Upper: Points not excluded by LEP and Tevatron data at the 95% CL. We show points currently excluded by the LHC with 1 fb^{-1} in green. The LHC exclusion reach for 5 and 15 fb^{-1} is shown in magenta and blue, while points outside the LHC Run-I reach are plotted in red (there are none here). Lower: Models that can be discovered (5σ) after 15 fb^{-1} of collected data. We include here those points that are currently excluded at less than 3σ (see text). We also indicate the discovery mode: $pp \rightarrow h \rightarrow WW$ (green), $pp \rightarrow h \rightarrow \gamma\gamma$ (magenta), $pp \rightarrow h/H/A \rightarrow \tau^+ \tau^-$ (blue). Note that the color code is different in the two plots.

As for the discovery prospects (right panel of Fig. 5), we observe that $h \rightarrow WW$ is an important discovery mode for lightest CP -even Higgs masses heavier than 120 GeV, and for CP -odd masses larger than 200 GeV, and that the inclusive tau channel is useful for discovery at $m_H < 325$ GeV. For light values of m_h (in the 115–130 GeV range) we have that the $\gamma\gamma$ channel becomes a discovery mode, playing a more important role than in the $\tan\beta = 2$ case. This is due to the enhancement of the Higgs signal in the diphoton channel, which in some cases can be as large as a factor of 8 above the SM. However, such a large diphoton signal is excluded by the current LHC dataset, that is able to test rates between 1.5–3 times the SM after combining the CMS and ATLAS limits. We note also that here the $H \rightarrow WW$ channel does not play a role, mainly due to the fact that in the large $\tan\beta$ regime the heavy CP -even Higgs coupling to electroweak vector bosons tends to be suppressed with respect to the SM value. We emphasize that essentially all the points in our scan for $\tan\beta = 20$ can be tested with 15 fb^{-1} . The couple of points marked as “not probed” in the left panel of Fig. 5 can actually be probed in the $\tau^+\tau^-$ channel at the 2σ level with the slightly larger luminosity of $\sim 16 \text{ fb}^{-1}$.

The LHC has great potential to discover Higgs bosons, but it is also possible to think of a scenario where, by the end of the 7 TeV LHC run, the SM Higgs would be excluded in the whole mass range, without any excess over the expectations in all search channels. In that case, almost all of our points for $\tan\beta = 2$ and $\tan\beta = 20$ would be excluded as well with 15 fb^{-1} . However, for intermediate values of $\tan\beta$, where the MSSM searches are less efficient and the search for h is more challenging (with m_h in the 114–120 GeV range), one would be left with a fraction of parameter space not probed with 15 fb^{-1} . Nevertheless, a sparse scan over $\tan\beta$ (using values of 4, 6 and 8) suggests that all such points can be probed with 20 fb^{-1} of integrated luminosity. We show these points in Fig. 6, in the $m_h - m_A$ plane, indicating the exclusion channel in each case: $pp \rightarrow h \rightarrow WW$ (green), $pp \rightarrow H \rightarrow \gamma\gamma$ (magenta), $Vh, h \rightarrow b\bar{b}$ (blue), $qqh, h \rightarrow \tau^+\tau^-$ (red) and $pp \rightarrow h \rightarrow \tau^+\tau^-$ (brown).

There are channels that have not yet been exploited by the experimental collaborations, e.g., $h \rightarrow AA, H \rightarrow hh$, or a charged Higgs search with suppressed $\text{BR}(H^+ \rightarrow \tau^+ \nu_\tau)$

B. Benchmark scenarios

Considering the summer 2011 LHC results we update the analysis of the BMSSM benchmark scenarios presented in Ref. [7] and introduce a number of additional points that illustrate the possibilities at the LHC with up to 15 fb^{-1} of data. We keep the notation of Ref. [7] for each point, labeling them from A to H, and show them as stars marked with the corresponding letter in Figs. 4 and 5.

We recall first our notation and conventions. The effective couplings squared, $g_{\phi X}^2$, are computed as the

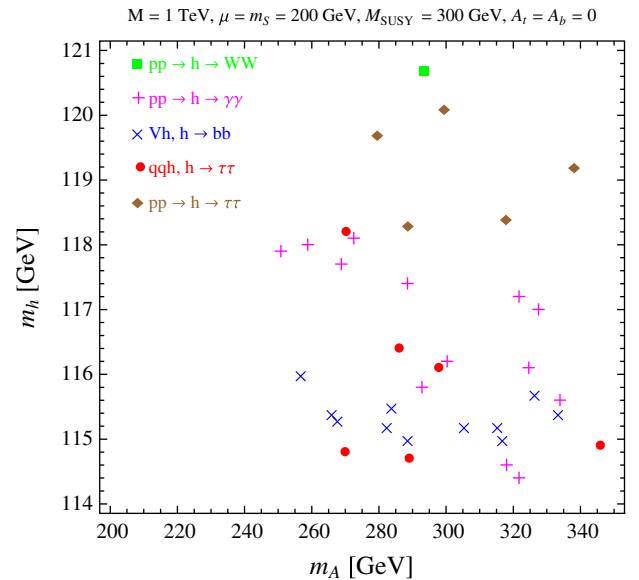


FIG. 6 (color online). Sparse scan over BMSSM scenarios, for $\tan\beta = 4, 6, 8$. We show only points that cannot be probed at the 2σ level at the 7 TeV LHC after 15 fb^{-1} per experiment of integrated luminosity. We indicate the discovery mode: $pp \rightarrow h \rightarrow WW$ (green), $pp \rightarrow h \rightarrow \gamma\gamma$ (magenta), $Vh, h \rightarrow b\bar{b}$ (blue), $qqh, h \rightarrow \tau^+\tau^-$ (red) and $pp \rightarrow h \rightarrow \tau^+\tau^-$ (brown).

ratio of the partial widths of the Higgs boson in our model to the SM ones, for $\phi \rightarrow X = gg, WW, \dots$. The effective cross section $g_{pp \rightarrow X}^2$, on the other hand, is defined as the ratio of the total *inclusive* cross section at the LHC in our model normalized to the SM result. The cross sections in our model are obtained by scaling each production mode with the corresponding effective coupling squared: $g_{\phi gg}^2$ for gluon fusion, $g_{\phi WW/ZZ}^2$ for the Higgs-strahlung and vector-boson fusion, and $g_{\phi b\bar{b}}^2/g_{\phi t\bar{t}}^2$ for the associated production with a bottom/top pair, respectively. We also define $Q_i(\mathcal{L})$ as the ratio between the signal (production cross section times branching fraction) in our model, in channel i , and the LHC 95% CL limit on this rate, at the luminosity \mathcal{L} . For each benchmark point, we will simply report the maximum value among all the Q_i . We will call by \mathcal{L}_2 and \mathcal{L}_5 the luminosities required to claim a 2σ exclusion (from now on, exclusion) or a 5σ discovery (from now on, discovery). For further details see Appendix B.

1. Benchmark scenarios for $\tan\beta = 2$

Of the six low- $\tan\beta$ benchmark points proposed in Ref. [7], four have been excluded at the $\sim 4\sigma$ level by the most recent LHC studies and two are not yet probed. The properties of these points (spectrum, couplings, branching ratios) were presented in [7]. For the excluded ones, here we simply summarize the exclusion channels and the associated significances. All these points are indicated by stars in the $m_H - m_h$ plane of Fig. 4:

Point B is excluded independently by the $pp \rightarrow h \rightarrow WW$ and $pp \rightarrow h \rightarrow \gamma\gamma$ LHC searches, both at the 4σ level. In fact, for this model, which has $m_h \approx 130$ GeV, the $pp \rightarrow h \rightarrow ZZ$ channel also excludes it at the 2.1σ level. The reason for such a high exclusion capability from LHC searches is a significant suppression in the $h \rightarrow b\bar{b}$ channel, that results in enhancements of 3.6, 2.7 and 3.5 w.r.t. SM rates in the WW , $\gamma\gamma$ and ZZ channels, respectively.

Point C is excluded by current data in the WW channel, with a statistical significance of 3.8σ (2.4σ) for h (H), that may be interpreted to give a combined exclusion at the 4.5σ level.

Point D is excluded independently by the $pp \rightarrow h \rightarrow WW/ZZ$ searches at the $2.5/3.3\sigma$ level, which yield a combined exclusion at the 4.1σ level.

Point E is excluded independently by the $pp \rightarrow h/H \rightarrow WW$ searches at the $2.1/1.9\sigma$ level, and by the $pp \rightarrow H \rightarrow ZZ$ search at the 2.7σ level, thus yielding a combined exclusion significance at the 3.9σ level.

One should notice that these points are strongly probed by the weak diboson channels. This is a rather direct consequence of the higher-dimension operators, which can have the following effects:

- (i) The lightest CP -even Higgs mass can increase sufficiently to make the WW , or even the ZZ decay modes sizable (or dominant).
- (ii) Both CP -even Higgs states can mix significantly so that they can *both* have sizable couplings to weak gauge boson pairs. Sometimes, it is the heavier CP -even state that couples dominantly to WW or ZZ .

These general observations imply that typically one or the other CP -even Higgs state (or in some cases both) is constrained by the SM Higgs searches in the above diboson channels. Such a situation is far less typical in the MSSM, where the lightest CP -even state decays dominantly into $b\bar{b}$ pairs, and would be searched for more efficiently in the $\gamma\gamma$ channel (although also in the MSSM, at low $\tan\beta$, the heavier CP -even H —while having a suppressed coupling to VV —can still have a sizable decay branching fraction into weak gauge bosons if its mass is in the appropriate kinematic range).

The left panel of Fig. 4 shows that most models with $m_h \geq 135$ GeV are excluded at least at the 2σ level by the most recent LHC searches. Furthermore, most of the remaining points will be probed with 5 fb^{-1} of integrated luminosity (combining both experiments), as shown by the magenta points in the same plot. The points not currently excluded will be tested mainly in the $h \rightarrow WW$ channel, but there are also many models where such a signal would actually correspond to the heavier CP -even Higgs. Finally, a few points will be tested in the $h \rightarrow \gamma\gamma$ channel; these have $m_h \approx 115$ – 118 GeV and $m_H > 220$ GeV (with very suppressed g_{HWW}^2). We show in Tables II, III, and IV representative examples of the models that can be probed

TABLE II. Masses and branching fractions in the BMSSM (and in the SM for h and H) for scenario A' . We only show the main decay modes. The rate of the most sensitive channel is normalized to the SM.

m_A (GeV)	POINT A'		
	m_h (GeV)	m_H (GeV)	m_{H^\pm} (GeV)
129	143	194	148
g_{hWW}^2	g_{HWW}^2	$g_{pp \rightarrow h}^2$	$g_{pp \rightarrow H}^2$
0.24	0.73	1.24	0.48
channel	BMSSM (SM)	channel	BMSSM (SM)
$h \rightarrow b\bar{b}$	0.62 (0.30)	$h \rightarrow WW$	0.21 (0.55)
$H \rightarrow WW$	0.74 (0.75)	$H \rightarrow ZZ$	0.24 (0.25)
$A \rightarrow b\bar{b}$	0.89	$A \rightarrow \tau\bar{\tau}$	0.10
$H^+ \rightarrow \bar{\tau}\nu_\tau$	0.82	$H^+ \rightarrow t\bar{b}$	0.15
$pp \rightarrow h \rightarrow WW$	$\mathcal{Q}(15 \text{ fb}^{-1})$	$\mathcal{L}_2 (\text{fb}^{-1})$	$\mathcal{L}_5 (\text{fb}^{-1})$
0.46	2.8	1.9	11.9

by the end of 2011 (i.e., assuming 5 fb^{-1} of integrated luminosity per experiment).

Other benchmark scenarios with neutral Higgs bosons decaying into diboson and requiring luminosities of order 10 fb^{-1} to be probed are present in our scan, and it would be interesting to explore these options in the case of no positive signals by the end of 2011.

Point A' in Table II corresponds to a model that can be excluded (discovered) in the $pp \rightarrow h \rightarrow WW$ channel with

TABLE III. Masses and branching fractions in the BMSSM for scenarios B' and C' . We only show the main decay modes. The rate of the most sensitive channel is normalized to the SM.

m_A (GeV)	POINT B'		
	m_h (GeV)	m_H (GeV)	m_{H^\pm} (GeV)
133	117	156	156
g_{hWW}^2	g_{HWW}^2	$g_{pp \rightarrow h}^2$	$g_{pp \rightarrow H}^2$
0.90	0.10	0.71	0.94
channel	BMSSM (SM)	channel	BMSSM (SM)
$h \rightarrow b\bar{b}$	0.84 (0.73)	$h \rightarrow \tau\bar{\tau}$	0.09 (0.08)
$H \rightarrow b\bar{b}$	0.64 (0.10)	$H \rightarrow \tau\bar{\tau}$	0.12 (0.01)
$H \rightarrow WW$	0.23 (0.80)	$A \rightarrow b\bar{b}/\tau\bar{\tau}$	0.89 / 0.10
$H^+ \rightarrow \bar{\tau}\nu_\tau$	0.72	$H^+ \rightarrow t\bar{b}$	0.24
$pp \rightarrow H \rightarrow WW$	$\mathcal{Q}(15 \text{ fb}^{-1})$	$\mathcal{L}_2 (\text{fb}^{-1})$	$\mathcal{L}_5 (\text{fb}^{-1})$
0.27	2.8	1.9	12.0

m_A (GeV)	POINT C'		
	m_h (GeV)	m_H (GeV)	m_{H^\pm} (GeV)
203	118	222	225
g_{hWW}^2	g_{HWW}^2	$g_{pp \rightarrow h}^2$	$g_{pp \rightarrow H}^2$
1.0	$\leq 10^{-3}$	1.22	0.4
channel	BMSSM (SM)	channel	BMSSM (SM)
$h \rightarrow b\bar{b}$	0.70 (0.72)	$h \rightarrow \tau\bar{\tau}$	0.07 (0.07)
$h \rightarrow WW$	0.13 (0.12)	$h \rightarrow \gamma\gamma (\times 10^{-3})$	2.1 (2.3)
$H \rightarrow b\bar{b}/\tau\bar{\tau}$	0.81/0.10	$H \rightarrow WW$	0.04
$A \rightarrow b\bar{b}/\tau\bar{\tau}$	0.87/0.10	$H^+ \rightarrow t\bar{b}$	1.0
$pp \rightarrow h \rightarrow \gamma\gamma$	$\mathcal{Q}(15 \text{ fb}^{-1})$	$\mathcal{L}_2 (\text{fb}^{-1})$	$\mathcal{L}_5 (\text{fb}^{-1})$
1.1	1.8	4.8	30

TABLE IV. Masses and branching fractions in the BMSSM for scenario F of Ref. [7]. The rate of the most sensitive channel is normalized to the SM.

POINT F			
$m_A(\text{GeV})$	$m_h(\text{GeV})$	$m_H(\text{GeV})$	$m_{H^\pm}(\text{GeV})$
64	135	155	125
$g_{hWW}^2 \leq 10^{-2}$	g_{HWW}^2	$g_{pp \rightarrow h}^2$	$g_{pp \rightarrow H}^2$
channel	BMSSM	channel	BMSSM
$h \rightarrow b\bar{b}$	0.15	$h \rightarrow AA$	0.84
$H \rightarrow WW$	0.12	$H \rightarrow AA$	0.84
$H \rightarrow b\bar{b}$	0.02	$A \rightarrow b\bar{b}/\tau\bar{\tau}$	0.91/0.09
$H^\pm \rightarrow \tau\nu_\tau$	0.56	$H^\pm \rightarrow W^\pm + A$	0.40
$pp \rightarrow H \rightarrow WW$	$\mathcal{L}(15 \text{ fb}^{-1})$	$\mathcal{L}_2 (\text{fb}^{-1})$	$\mathcal{L}_5 (\text{fb}^{-1})$
0.18	1.8	4.9	30

1.9(11.9) fb^{-1} . Note that in this case, it is actually the heavy CP -even Higgs H that couples more strongly to the gauge bosons. With a mass of $m_H \approx 194 \text{ GeV}$, the model can be excluded independently at the 95% CL in the $pp \rightarrow H \rightarrow WW$ and $pp \rightarrow H \rightarrow ZZ$ channels, with $\mathcal{L} \approx 2.6 \text{ fb}^{-1}$ and $\mathcal{L} \approx 4.5 \text{ fb}^{-1}$, respectively. On the other hand, a discovery in these two channels could be obtained with $\mathcal{L} \approx 16 \text{ fb}^{-1}$ and $\mathcal{L} \approx 28 \text{ fb}^{-1}$, respectively.

Point B' in the upper part of Table III corresponds to a model that can be excluded (discovered) in the $pp \rightarrow H \rightarrow WW$ channel with 1.9(12) fb^{-1} : although the heavy CP -even Higgs H has a suppressed coupling to W -pairs, the $\text{BR}(WW)$ is non-negligible, while the production is slightly reduced with respect to the SM. The CP -even Higgs boson h can be probed at the 2σ level with $\mathcal{L} \approx 22 \text{ fb}^{-1}$ in the Vh , $h \rightarrow b\bar{b}$ and in the $q\bar{q}h$, $h \rightarrow \tau^+\tau^-$ channels.

Point C' in the lower part of Table III corresponds to a model that can be excluded (discovered) in the $pp \rightarrow h \rightarrow \gamma\gamma$ channel with 4.8(30) fb^{-1} , and in the $pp \rightarrow h \rightarrow WW$ channel with 6.1(38) fb^{-1} . In this example h is essentially SM-like, although it presents some enhancement in production compared to a SM Higgs. The remaining Higgs bosons are likely hard to discover at the LHC Run-I in this low $\tan\beta$ scenario. For instance, for the pseudoscalar Higgs A , one would need 23 fb^{-1} for a 2σ exclusion in the $\tau^+\tau^-$ channel.

Point F is one of the benchmark points presented in Ref. [7] that have not been excluded (see Table IV).⁶ It has a rather light pseudoscalar Higgs, so that both $\text{BR}(h/H \rightarrow AA)$ are sizable. Therefore, possible search channels could be $b\bar{b}b\bar{b}$, $b\bar{b}\tau^+\tau^-$, or $\tau^+\tau^-\tau^+\tau^-$. Aside

⁶The other point at low $\tan\beta$ of Ref. [7] that has not been excluded was labeled *A* in that reference. It has MSSM-like characteristics, with a SM-like Higgs with $m_h \approx 118 \text{ GeV}$ that could be excluded (discovered) in the $\gamma\gamma$ channel with 14(90) fb^{-1} . The nonstandard Higgs bosons have masses of about 240 GeV, and are harder to find at the LHC.

from these options, which we are not considering here, the model can be excluded (discovered) in the $pp \rightarrow H \rightarrow WW$ channel with 4.9(30) fb^{-1} . The charged Higgs search cannot be applied in a straightforward manner, since $\text{BR}(H^\pm \rightarrow \tau^+\nu_\tau) = 0.56$. A new interesting decay mode for the charged Higgs opens up in this case: $H^\pm \rightarrow W^\pm A$.

Finally, there are a couple of low- $\tan\beta$ models labeled in the left panel of Fig. 4 as “not probed” (red points). In some cases, this is due to the presence of a relatively light CP -odd Higgs that provides an additional decay channel for h and/or H , which suppresses the signal in the channels probed so far, thus making them ineffective even with 15 fb^{-1} . In other cases, the BR into $b\bar{b}$ presents an enhancement that also has the effect of reducing the signal in the most sensitive channels. However, we find that all such models have a relatively light charged Higgs ($\sim 115\text{--}130 \text{ GeV}$) with a non-negligible branching ratio into $\tau\nu_\tau$, and we expect that the $H^\pm \rightarrow \tau\nu_\tau$ channel should be effective in discovering such a state. However, the published analyses do not apply in a straightforward way since here $\text{BR}(H^\pm \rightarrow \tau^+\nu_\tau) \neq 1$, being diluted by the $H^\pm \rightarrow W^\pm A$ decay channel.

2. Benchmark scenarios for $\tan\beta = 20$

The two $\tan\beta = 20$ benchmark points that were defined in Ref. [7] have been excluded as follows:

Point G is excluded by the $pp \rightarrow h \rightarrow WW$ searches at the 2.6σ level.

Point H is excluded by the $pp \rightarrow h \rightarrow \gamma\gamma$ searches at the 5.8σ level.

We see in the right panel of Fig. 5 that the most sensitive channels are $pp \rightarrow h \rightarrow WW$, $pp \rightarrow h \rightarrow \gamma\gamma$ and $pp \rightarrow h/H/A \rightarrow \tau^+\tau^-$ (at large $\tan\beta$ the HVV couplings are always suppressed). We select here additional benchmark points, illustrating the above cases. These are models that are presently allowed and can be discovered with $\mathcal{L} = 15 \text{ fb}^{-1}$:

Point J in Table V corresponds to a model that can be excluded (discovered) in the $pp \rightarrow h \rightarrow WW$ channel with about 2(13) fb^{-1} . It can also be excluded (discovered) in $h \rightarrow \gamma\gamma$ with 8(52) fb^{-1} . Note that it has an enhanced branching ratio into τ pairs (and $b\bar{b}$) compared to the SM, and can be excluded (discovered) with 4.2(26) fb^{-1} in this channel. The nonstandard Higgs bosons (around 300 GeV) can be excluded (discovered) in the $\tau^+\tau^-$ channel with 5.1(32) fb^{-1} for A and 10.2(63) fb^{-1} for H . Combining their signals, a total integrated luminosity of 3.4(21) fb^{-1} is required for exclusion (discovery). We also note that since $\text{BR}(H \rightarrow hh) \approx 0.13$, one could also look for H by studying the $b\bar{b}\gamma\gamma$, $b\bar{b}b\bar{b}$, $b\bar{b}\tau^+\tau^-$, $\tau^+\tau^-\tau^+\tau^-$ or even $b\bar{b}W^+W^-$. Dedicated studies would be necessary to access the viability of these decay channels.

Point K in Table VI corresponds to a model that can be excluded (discovered) in the $pp \rightarrow h \rightarrow \gamma\gamma$ channel with 2.1(13) fb^{-1} . The nonstandard Higgs bosons (around 380 GeV) can be excluded (discovered) in the $\tau^+\tau^-$ channel

TABLE V. Masses and branching fractions in the BMSSM (and in the SM for h) for scenario J . We only show the main decay modes. The rate of the most sensitive channel is normalized to the SM.

POINT J			
m_A (GeV)	m_h (GeV)	m_H (GeV)	m_{H^\pm} (GeV)
302	129	312	305
g_{hWW}^2	g_{HWW}^2	$g_{pp\rightarrow h}^2$	$g_{pp\rightarrow H}^2$
0.97	0.02	1.55	0.62
channel	BMSSM (SM)	channel	BMSSM (SM)
$h \rightarrow b\bar{b}$	0.65 (0.56)	$h \rightarrow \tau\bar{\tau}$	0.11 (0.06)
$h \rightarrow WW$	0.16 (0.27)	$H \rightarrow b\bar{b}/\tau\bar{\tau}$	0.65 / 0.11
$H \rightarrow hh$	0.13	$A \rightarrow b\bar{b}/\tau\bar{\tau}$	0.81 / 0.14
$H^+ \rightarrow \bar{\tau}\nu_\tau$	0.20	$H^+ \rightarrow t\bar{b}$	0.75
$pp \rightarrow h \rightarrow WW$	$\mathcal{Q}(15 \text{ fb}^{-1})$	\mathcal{L}_2 (fb $^{-1}$)	\mathcal{L}_5 (fb $^{-1}$)
0.93	2.7	2.1	13.1

TABLE VI. Masses and branching fractions in the BMSSM (and in the SM for h) for scenario K . We only show the main decay modes. The rate of the most sensitive channel is normalized to the SM.

POINT K			
m_A (GeV)	m_h (GeV)	m_H (GeV)	m_{H^\pm} (GeV)
382	115	375	388
g_{hWW}^2	g_{HWW}^2	$g_{pp\rightarrow h}^2$	$g_{pp\rightarrow H}^2$
0.99	$<10^{-3}$	1.22	0.28
channel	BMSSM (SM)	channel	BMSSM (SM)
$h \rightarrow b\bar{b}$	0.65 (0.75)	$h \rightarrow \tau\bar{\tau}$	0.06 (0.08)
$h \rightarrow WW$	0.14 (0.08)	$H \rightarrow b\bar{b}/\tau\bar{\tau}$	0.78/0.14
$A \rightarrow b\bar{b}$	0.69	$A \rightarrow \tau\bar{\tau}$	0.12
$H^+ \rightarrow \bar{\tau}\nu_\tau$	0.16	$H^+ \rightarrow t\bar{b}$	0.74
$pp \rightarrow h \rightarrow \gamma\gamma$	$\mathcal{Q}(15 \text{ fb}^{-1})$	\mathcal{L}_2 (fb $^{-1}$)	\mathcal{L}_5 (fb $^{-1}$)
1.8	2.7	2.1	13

with $6.3(39) \text{ fb}^{-1}$ (we add their signals since their mass difference is less than 10 GeV).

Point L in Table VII illustrates models that can be mainly tested in the $\tau^+\tau^-$ channel. We note that in such model points only one neutral Higgs boson can be discovered (in the $\tau^+\tau^-$ channel) in the 7 TeV LHC run with about 15 fb^{-1} . In this example, the pseudoscalar Higgs A can be excluded (discovered) with $2.2(13.7) \text{ fb}^{-1}$, while h and H would require about 3.5 and 5.9 fb^{-1} for a 2σ excess and more than 20 fb^{-1} for 5σ , respectively. In this case, h can also be probed by the WW channel, which requires $3.6(22.2) \text{ fb}^{-1}$ for exclusion (discovery).

Before closing this subsection, we would like to stress the fact that in our $\tan\beta = 20$ scan there are points where the lightest CP -even Higgs boson h will be probed with $\mathcal{O}(10 \text{ fb}^{-1})$ in the WW or $\gamma\gamma$ decay modes, and also points where either h , H or A can be tested in the $\tau^+\tau^-$ channel with a similar luminosity. Those possibilities would be very interesting in the absence of any positive signal with the recently collected $\mathcal{O}(5 \text{ fb}^{-1})$ data sample.

TABLE VII. Masses and branching fractions in the BMSSM (and in the SM for h) for scenario L . We only show the main decay modes.

POINT L			
m_A (GeV)	m_h (GeV)	m_H (GeV)	m_{H^\pm} (GeV)
256	129	278	275
g_{hWW}^2	g_{HWW}^2	$g_{pp\rightarrow h}^2$	$g_{pp\rightarrow H}^2$
0.99	0.02	1.6	0.86
channel	BMSSM (SM)	channel	BMSSM (SM)
$h \rightarrow b\bar{b}$	0.70 (0.56)	$h \rightarrow \tau\bar{\tau}$	0.12 (0.06)
$h \rightarrow WW$	0.12 (0.28)	$H \rightarrow b\bar{b}/\tau\bar{\tau}$	0.68/0.11
$H \rightarrow hh$	0.13	$A \rightarrow b\bar{b}/\tau\bar{\tau}$	0.85/0.14
$H^+ \rightarrow \bar{\tau}\nu_\tau$	0.22	$H^+ \rightarrow t\bar{b}$	0.73
$\sigma(pp \rightarrow X \rightarrow \tau\bar{\tau})$ (pb)	$\mathcal{Q}(15 \text{ fb}^{-1})$	\mathcal{L}_2 (fb $^{-1}$)	\mathcal{L}_5 (fb $^{-1}$)
A : 0.6	2.6	2.2	13.7
H : 0.3	1.6	5.9	37
h : 2.9	2.1	3.5	22.0

3. Benchmark scenarios for intermediate $\tan\beta$

These scenarios can be probed with about 20 fb^{-1} of integrated luminosity in the individual Vh , $h \rightarrow b\bar{b}$, qqh , $h \rightarrow \tau^+\tau^-$, or $pp \rightarrow h \rightarrow \gamma\gamma$ channels. The $pp \rightarrow H/A \rightarrow \tau^+\tau^-$ searches are less effective due to the moderate value of $\tan\beta$, and in some cases the nonstandard Higgs bosons may remain beyond the LHC reach. However, we point out that when kinematically open, the $H \rightarrow hh$ channel can have a sizable branching fraction, thus giving a potential handle on the extended Higgs sector (beyond the SM-like Higgs). By contrast, this can happen in the MSSM only for significantly smaller values of $\tan\beta$, and would point to the presence of heavy physics, as studied here. As an illustration of a ‘‘more challenging’’ scenario, we present:

Point M in Table VIII, which illustrates intermediate $\tan\beta$ (~ 6) models that require more than 15 fb^{-1} for

TABLE VIII. Masses and branching fractions in the BMSSM (and in the SM for h) for scenario M . We only show the main decay modes.

POINT M			
m_A (GeV)	m_h (GeV)	m_H (GeV)	m_{H^\pm} (GeV)
200	115	193	203
g_{hWW}^2	g_{HWW}^2	$g_{pp\rightarrow h}^2$	$g_{pp\rightarrow H}^2$
0.99	$\leq 10^{-2}$	1.12	0.37
channel	BMSSM (SM)	channel	BMSSM (SM)
$h \rightarrow b\bar{b}$	0.82 (0.75)	$h \rightarrow \tau\bar{\tau}$	0.09 (0.08)
$h \rightarrow WW$	0.05 (0.09)	$H \rightarrow b\bar{b}/\tau\bar{\tau}$	0.85/0.11
$A \rightarrow b\bar{b}/\tau\bar{\tau}$	0.88/0.12	$H^+ \rightarrow \bar{\tau}\nu_\tau/t\bar{b}$	0.25/0.74
$Vh, h \rightarrow b\bar{b}$	$\mathcal{Q}(15 \text{ fb}^{-1})$	\mathcal{L}_2 (fb $^{-1}$)	\mathcal{L}_5 (fb $^{-1}$)
1.08	0.98	15.6	98
$qqh, h \rightarrow \tau\bar{\tau}$	$\mathcal{Q}(15 \text{ fb}^{-1})$	\mathcal{L}_2 (fb $^{-1}$)	\mathcal{L}_5 (fb $^{-1}$)
1.12	0.94	17	106
$pp \rightarrow h \rightarrow \gamma\gamma$	$\mathcal{Q}(15 \text{ fb}^{-1})$	\mathcal{L}_2 (fb $^{-1}$)	\mathcal{L}_5 (fb $^{-1}$)
0.56	0.83	22	137

exclusion (we have allowed here for $A_t = A_b = 300$ GeV, keeping $M_{\text{SUSY}} = 300$ GeV). Note that the diphoton channel is suppressed by a factor of almost 2 compared to the SM, and would require $\sim 20 \text{ fb}^{-1}$ for exclusion. The lightest CP -even Higgs could be excluded earlier in the Vh , $h \rightarrow b\bar{b}$ or qqh , $h \rightarrow \tau\tau$ channels with $\sim 16 \text{ fb}^{-1}$ and $\sim 17 \text{ fb}^{-1}$, respectively. However, naively combining the three search channels one could achieve exclusion with only $\sim 6 \text{ fb}^{-1}$.

IV. APPLICATION TO SPECIFIC UV THEORIES

The analysis of the previous sections relies solely on the inclusion of higher-dimension operators involving the MSSM Higgses (H_u and H_d) in the super- and Kähler potentials, suppressed by up to $1/M^2$, where M is the scale of the physics being integrated out. As mentioned in the introduction, our formalism assumes that these are nearly supersymmetric thresholds, thus treating SUSY breaking in the heavy sector as a perturbation (included via a spurion superfield). We emphasized in Ref. [6] that the generic EFT operators can be obtained from extensions of the MSSM involving massive singlet and triplet superfields, as well as massive gauge fields (W' and/or Z'). However, there are two classes of operators that seem hard to induce at tree level [those with coefficients proportional to c_6 and c_7 in Eq. (3)], but that are allowed by supersymmetry. Although we allowed in our scan that all of these operators have order-one coefficients, it often happens that turning off c_6 and c_7 results in changes to the spectrum that are within the uncertainties expected in the EFT. One can therefore get an idea of the type of new physics that could be associated with a given EFT benchmark point by using the relations derived in [6] between such UV examples and the EFT. We have done this explicitly for the benchmark points of the previous section, and present some of the details (and caveats) in Appendix A. This serves as a “proof of existence” that the qualitative physics studied within the EFT can be obtained in specific (even if complicated) UV completions.⁷

In this section we illustrate a somewhat orthogonal aspect. We focus on specific “simple” UV extensions of the MSSM, and perform a study of the corresponding bounds from the 7 TeV run of the LHC, within the EFT framework. In these cases, we can further analyze the physics in the full model (e.g., the spectrum), and in this way quantify the uncertainties in the EFT. We will focus on two classes of models: extensions by a massive singlet, and extensions by massive $SU(2)_L$ triplets. We do not consider gauge extensions, since they necessitate adding a suitable

sector that breaks the extended gauge symmetry to the SM one, and this sector can give further contributions to the EFT operators. Although such an analysis could be done in principle, the results would be much more model-dependent. At any rate, we find that the EFT is in good agreement with the predictions of the UV theory in the simpler cases we analyze in the following two subsections, which provides confidence for the generic EFT results.

A. Singlet models

Consider a model where the MSSM is extended by a singlet superfield, S , with the following superpotential (apart from the standard Yukawa interactions)⁸:

$$W = \mu H_u H_d - \frac{1}{2} M S^2 + \lambda_S S H_u H_d - X \left(\frac{1}{2} a_2 M S^2 + a_3 \lambda_S S H_u H_d \right), \quad (6)$$

where a_2 and a_3 are dimensionless, and $X = m_s \theta^2$ is a (dimensionless) spurion superfield parametrizing SUSY breaking in the singlet sector. We also add the usual non-holomorphic masses for H_u , H_d and S (the latter taken to be m_s^2), as well as the standard b -term. Integrating out S at tree level induces the following coefficients in the effective theory (see Eq. (3) and Ref. [6] for the definitions of the coefficients in the EFT, ω_1 , α_1 , c_i , γ_i , β_i):

$$\begin{aligned} \omega_1 &= \lambda_S^2, & \alpha_1 &= a_2 - 2a_3, & c_4 &= |\lambda_S|^2, \\ \gamma_4 &= a_2 - a_3, & \beta_4 &= |a_2 - a_3|^2 - 1. \end{aligned} \quad (7)$$

We have scanned over λ_S , a_2 and a_3 (allowing λ_S to be as large as 1.5), and performed the EFT checks described in [6] (i.e., those used in the generic analysis of Sec. III). We have also fixed the SUSY spectrum (the parameter M_{SUSY} describing the stop sector) as in the previous section. It is worth noting that such a setup for the μ term and SUSY masses can be achieved [51] in singlet extensions of the MSSM with extra discrete symmetries [52].

The results for $\tan\beta = 2$ are shown in the left panel of Fig. 7, showing the power of the current LHC bounds and the projections for 5 and 15 fb^{-1} of integrated luminosity. We see that the pattern is qualitatively similar to the one displayed in the model-independent analysis of Sec. III (here we scanned up to $m_A = 300$ GeV). In the plot we have explicitly excluded a number of points with a light CP -odd Higgs (such that either $h \rightarrow AA$ or $H \rightarrow AA$ are kinematically allowed) for the reasons explained in the next paragraph.

We have also analyzed exactly the spectrum of states without integrating out the singlet. The comparison to the EFT spectrum is performed by requiring that $v = 174$ GeV, $\tan\beta$ and m_{H^\pm} match in the effective and full

⁷Such UV completions may in turn have Landau poles at some intermediate scale, which would indicate the presence of additional, much heavier physics. Such issues do not concern us in this work, since their effects on the Higgs sector can be expected to be suppressed.

⁸For convenience in the numerical analysis we have flipped the sign of M compared to Ref. [6].

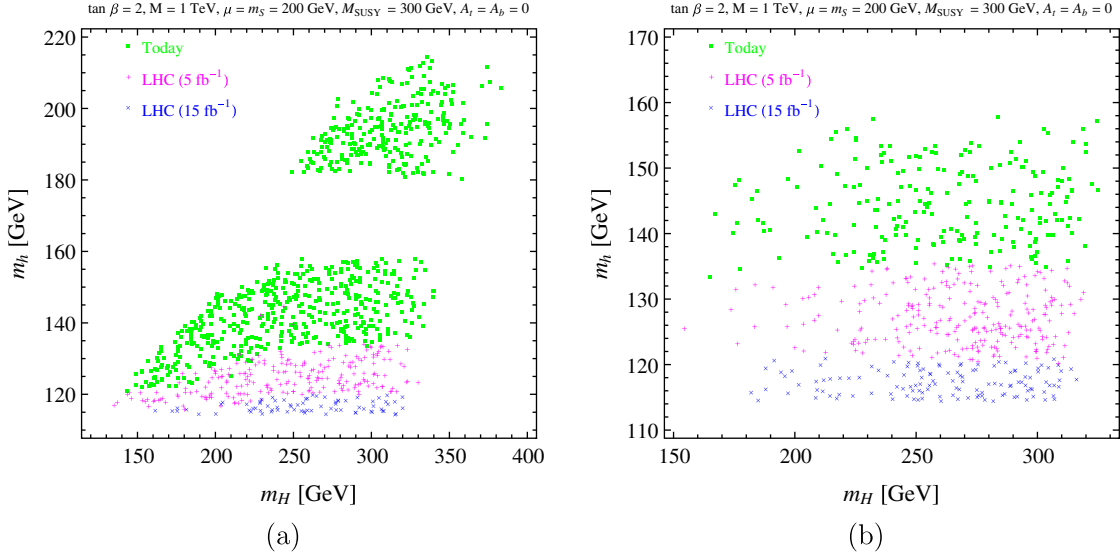


FIG. 7 (color online). Left panel: scan over parameter points in the singlet theory of Eq. (6), showing the current LHC sensitivity and projections for the 7 TeV LHC run. Right panel: scan corresponding to a theory extended by $SU(2)_L$ triplets, as defined in Eq. (8), showing the current LHC sensitivity and projections for the 7 TeV LHC run. Both examples correspond to $\tan\beta = 2$.

theories (by adjusting $m_{H_u}^2$, $m_{H_d}^2$ and b). All other parameters (μ , M , λ_S , a_2 , a_3 , and M_{SUSY}) are kept fixed. We choose to match onto the charged Higgs mass (as opposed to m_A , for instance) because the charged sector is common to both theories, and the comparison is therefore cleaner. We find that typically the agreement in m_h is within 10% and in m_H it is within a few percent. The largest discrepancies appear in m_A when this state is light, and can reach order 30%. One should then take into account that points where m_A is sufficiently light that the $h \rightarrow AA$ channel is open within the EFT, might get corrections that can change this conclusion. Except in such extreme cases (a relatively small number of points), the uncertainties are as expected in the EFT analysis. However, we note that in certain regions a 10% variation in m_h can be relevant phenomenologically. Such a change can nevertheless be compensated by radiative corrections, without affecting too strongly the other Higgs bosons, and therefore the phenomenological conclusions for the generic EFT points in our sample can be reasonably obtained within a singlet extension. Thus, except possibly for parameter points with “light” states, we conclude from this exercise that the analysis based on the EFT is reliable. In particular, we trust the results for the MSSM Higgs sector effective couplings which is much harder to analyze in the full theory (and is one place where the EFT analysis shows its power).

B. Extensions with Triplets

Now we consider an extension by $SU(2)_L$ triplets. Specifically, we include a triplet \tilde{T} , with hypercharge $Y = 0$, and a vectorlike pair T and \bar{T} , with hypercharges

$Y = -1$ and $Y = +1$, respectively. The superpotential is⁹

$$\begin{aligned}
 W = & \mu H_u H_d - \frac{1}{2} M_{\tilde{T}} \tilde{T}^a \tilde{T}^a + M_T T^a \bar{T}^a \\
 & + \tilde{\lambda}_T H_u \tilde{T} H_d + \frac{1}{2} \lambda_T H_u T H_u + \frac{1}{2} \lambda_{\bar{T}} H_d \bar{T} H_d \\
 & - X \left(\frac{1}{2} \tilde{a}_2 M_{\tilde{T}} \tilde{T}^a \tilde{T}^a + \tilde{a}_3 \tilde{\lambda}_T H_u \tilde{T} H_d + a_2 M_T T^a \bar{T}^a \right. \\
 & \left. + \frac{1}{2} a_3 \lambda_T H_u T H_u + \frac{1}{2} a_4 \lambda_{\bar{T}} H_d \bar{T} H_d \right), \quad (8)
 \end{aligned}$$

together with nonholomorphic masses for H_u , H_d , \tilde{T} , T and \bar{T} . In our scan we will take the soft masses for all the triplets to be given by m_S^2 . The reason we include the various triplets simultaneously is that the $Y = 0$ triplet contributes to the Peskin-Takeuchi T -parameter with opposite sign to the vectorlike pair with $Y = \pm 1$ (the former contribution is positive while the latter are negative). As a result there can naturally exist partial cancellations in the T -parameter that can allow the parameters to be larger and affect the MSSM Higgs sector more significantly.

To second order in $1/M_{\tilde{T}} \sim 1/M_T$ the contributions to the EFT operators generated by integrating out the triplets are simply additive, and were given in [6]. Assuming, for concreteness, that $M_T = M_{\tilde{T}}$, and following the notation introduced in Ref. [6] and summarized around Eq. (3), the following coefficients in the EFT are induced:

⁹Note that, due to the factor of 1/2 in $T \equiv T^a \tau^a$, etc., the normalizations of the Yukawa couplings are such that one should “compare” $\lambda_{\tilde{T}}/2$, $\lambda_T/2$ and $\lambda_{\bar{T}}/2$ to the singlet coupling λ_S of the previous subsection.

$$\begin{aligned}
M &= M_T = M_{\tilde{T}}, & \omega_1 &= \frac{1}{4}\tilde{\lambda}_T^2 + \frac{1}{4}\lambda_T\lambda_{\tilde{T}}, \\
\alpha_1 &= \tilde{a}_2 - 2\tilde{a}_3 + a_2 - a_3 - a_4, & c_1 &= \frac{1}{4}\lambda_{\tilde{T}}^2, \\
\gamma_1 &= a_2 - a_4, & \beta_1 &= |a_2 - a_4|^2 - 1, \\
c_2 &= \frac{1}{4}\lambda_{\tilde{T}}^2, & \gamma_2 &= a_2 - a_3, & \beta_2 &= |a_2 - a_3|^2 - 1, \\
c_3 &= \frac{1}{2}|\tilde{\lambda}_T|^2, & \gamma_3 &= \tilde{a}_2 - \tilde{a}_3, & \beta_3 &= |\tilde{a}_2 - \tilde{a}_3|^2 - 1, \\
c_4 &= -\frac{1}{4}|\tilde{\lambda}_T|^2, & \gamma_4 &= \tilde{a}_2 - \tilde{a}_3, & \beta_4 &= |\tilde{a}_2 - \tilde{a}_3|^2 - 1.
\end{aligned} \tag{9}$$

We have scanned over $\lambda_{\tilde{T}}$, λ_T , $\lambda_{\tilde{T}}$, \tilde{a}_2 , \tilde{a}_3 , a_2 , a_3 and a_4 (again allowing the λ_i 's to be as large as 1.5). However, we keep only points such that $\omega_1 < 2$ and $\alpha_1 < 1.5$ so as to remain within the perturbative regime in the EFT. We performed again the EFT checks described in [6], which include checking consistency with electroweak precision tests (EWPT), allowing for a potential contribution to the oblique parameters from the SUSY sector, e.g., from splittings in the slepton doublets. We have also fixed the SUSY spectrum as in the previous section (and as in the singlet model above). The results for $\tan\beta = 2$ are shown in the right panel of Fig. 7, showing the power of the current LHC bounds and the projections for 5 and 15 fb^{-1} of integrated luminosity. Again, we see that the pattern is qualitatively similar to the one displayed in the model-independent analysis of Sec. III, except that m_h reaches only values of order 160 GeV (for the range of parameters described above). The scan here corresponds to $70 \text{ GeV} < m_A < 300 \text{ GeV}$.

As in the case of the singlet model, we have compared the EFT predictions to the exact spectrum for Eq. (8). We match again to v , $\tan\beta$ and m_{H^\pm} by adjusting $m_{H_u}^2$, $m_{H_d}^2$ and b . All other parameters (μ , M , $\lambda_{\tilde{T}}$, λ_T , $\lambda_{\tilde{T}}$, \tilde{a}_2 , \tilde{a}_3 , a_2 , a_3 , a_4 , and M_{SUSY}) are kept fixed. We find that for the bulk of the scanned points the agreement is within 10%,¹⁰ and often much better. Therefore, as for the singlet theory, we conclude that the EFT analysis captures the physics of the triplet model reliably.

V. CONCLUSIONS

In this work we have analyzed the current LHC constraints on a large class of extended Higgs sectors in supersymmetric theories, where the physics beyond the MSSM (assumed to be approximately supersymmetric) is somewhat heavier than the MSSM Higgs degrees of freedom. In order to perform a relatively model-independent study, we have parametrized the effects of the extended sector on the

MSSM Higgs bosons via higher-dimension operators. We consider operators up to dimension-six in the superpotential and Kähler potential, which were shown in Ref. [6] to be potentially very relevant in determining the phenomenology of the Higgs sector. In particular, it was shown in [7] that the SUSY Higgs signals could be markedly different from the standard expectations built on the MSSM intuition. The profound distortion of the two-Higgs doublet sector could have led to striking signals during the very early LHC era. However, as shown in this work, such scenarios are now highly constrained by the current null results from the LHC Higgs searches, based on about $1\text{--}2 \text{ fb}^{-1}$ of integrated luminosity.

This does not mean that extended SUSY Higgs sectors are close to being ruled out, but it suggests that the Higgs phenomenology will likely be similar to the MSSM one, with a light CP -even Higgs decaying dominantly into bottom pairs, that can be searched for more effectively in the diphoton or W^+W^- channel (depending on its mass), and perhaps in the $\tau^+\tau^-$ channel. Of course, nonstandard decays into new light states, not considered in this work, remain also as a possibility. The nonstandard Higgs bosons will likely have suppressed couplings to the weak gauge bosons, and be somewhat harder to discover unless $\tan\beta$ is relatively large. Nevertheless, here can still exist interesting decays such as $H \rightarrow hh$ (that are typically suppressed in the MSSM, unless $\tan\beta$ is small and in some tension with the Higgs LEP bound), that can occur with a sizable branching fraction as a result of the presence of the heavy physics. Such a signal could indicate the presence of BMSSM physics that could be connected to additional contributions to the mass of the lightest CP -even, SM-like Higgs state, that may alleviate the tensions present in the MSSM, as also discussed recently within specific UV extensions of the MSSM in [53,54]. We have also analyzed here, within the effective theory formalism, specific theories involving additional singlets or $SU(2)_L$ triplets, and verified that the EFT analysis can indeed provide a reasonable approximation in such cases. It is found that the qualitative conclusions are similar to those obtained without the prejudice of specific UV theories.

Finally, we have presented projections for 5 and 15 fb^{-1} of integrated luminosity (roughly anticipating the situation by the end of 2011, and by the end of the 7 TeV run of the LHC, respectively), taking into account the possible combination of ATLAS and CMS results in each of the relevant search channels. We find that at both low (i.e., order one) and large $\tan\beta$, such amount of data can either exclude a very large region of parameter space, or make a discovery. We also point out that if the SM Higgs is excluded over the whole mass range, this may be an indication of a Higgs with a mass close to the LEP bound and an enhancement in the $b\bar{b}$ channel, as can happen both in the MSSM and in some extensions of the type studied in this work. Nevertheless, we expect that if supersymmetry is relevant

¹⁰In some cases, the EFT can overestimate m_h by as much as 10%, which can easily be compensated by radiative corrections, so that the phenomenological conclusions remain valid.

at the weak scale, signals from its Higgs sector are likely to appear over the next few years.

ACKNOWLEDGMENTS

We thank Patrick Draper and Carlos Wagner for useful discussions. Fermilab is operated by Fermi Research Alliance, LLC, under Contract No. DE-AC02-07CH11359 with the U. S. Department of Energy. E. P. is supported by the DOE Grant No. DE-FG02-92ER40699. J.Z. is supported by the Swiss National Science Foundation (SNF) under Contract No. 200020-138206. This work was supported by the Research Executive Agency (REA) of the European Union under the Grant Agreement No. PITN-GA-2010-264564 (LHCPhenoNet). M.C. would like to thank the Aspen Center for Physics, where part of this work has been done.

Note added.—While this article was being considered for publication, the ATLAS and CMS collaborations presented the results from updated Higgs searches based on a dataset of about 5 fb^{-1} . Interestingly, their analysis hints to a possible Higgs signal at around 125 GeV. The production rates in the WW , ZZ and diphoton channels would be compatible with a SM Higgs, although moderate deviations are also compatible with the data. If the excess was indeed a true Higgs signal it could easily be accommodated by models within our parameter scan. We find many points such that the lightest CP -even Higgs has a mass in the 123–127 GeV range, while the rates in all three gauge boson decay channels are standard-model-like. Some models also exhibit order one, but correlated, enhancements or suppressions with respect to a SM Higgs in the above channels.

APPENDIX A: BENCHMARK POINTS AND UV COMPLETIONS

In this appendix we establish a connection between the generic scan over parameters in the EFT, and possible UV completions that could give rise to such effects. We illustrate the point with the benchmark models of Sec. III. As mentioned in Sec. IV, we can reproduce most of the EFT coefficients by a combination of massive singlets and triplets, as in the models of Secs. IV A and IV B, plus a massive W' with gauge coupling \tilde{g} and a massive Z' with gauge coupling g' . For additional details on the EFT operators induced by these gauge extensions, we refer the reader to our previous work [6]. In such gauge extensions, there can exist additional contributions to the EFT operators from the sector that breaks the extended gauge symmetry to the SM one, if that sector interacts with the MSSM Higgs fields in any relevant way. To be definite, we will assume that any such couplings are subdominant, since our point here is to *illustrate* that specific generic benchmark models can actually be obtained from a well-defined theory. Note that additional contributions give more freedom to obtain a given set of EFT coefficients, so allowing such couplings

would only strengthen our point. However, there are a number of issues that should be taken into consideration:

- (i) The coefficients proportional to c_6 and c_7 cannot be easily obtained at tree level, although we have allowed them with order-one strength in our scan (they are certainly allowed by the symmetries). Nevertheless, often their effects do not change the qualitative features, e.g., they do not induce changes larger than the uncertainties already expected in the EFT approximation (especially at low $\tan\beta$; at large $\tan\beta$ they can be more important). Also, sometimes those changes can be partially compensated by other, unrelated effects such as somewhat different radiative corrections. Thus, it is still interesting to specify what kind of physics could generate the operators other than those associated with c_6 and c_7 .
- (ii) Besides a sector that breaks the extended gauge symmetry to the SM, in the case of $U(1)'$ additional matter may be necessary to cancel anomalies. We do not address this issue here, but note that the additional matter (probably with masses of order M) can give additional contributions to the EFT operators, again allowing additional freedom in generating the given EFT coefficients. However, for illustration purposes, we will assume that the possible couplings of these fields to the MSSM Higgs bosons are small.
- (iii) In principle, the different “heavy” fields can have somewhat different masses. For concreteness, here we will assume a common (SUSY) mass M for all the heavy states.

In Table IX we give examples of values of parameters in UV completions with the above ingredients (singlets, triplets and gauge extensions) that reproduce all coefficients of the benchmark scenarios shown in Sec. III that have not been excluded by current collider data, except for c_6 and c_7 (whose values we also list). There are more UV parameters than those in the EFT and therefore some amount of redundancy is present. We have arbitrarily fixed the $U(1)'$ charges of H_u and H_d (denoted by Q_u and Q_d in the tables), as well as the $U(1)'$ gauge coupling g' . We do not exhibit the parameters associated with SUSY-breaking operators, but there is more than enough freedom in the UV theory to accommodate those. It turns out that in most of these benchmark points one could turn off c_6 and c_7 without changing the conclusions. An exception is illustrated by Point K, where these operators give a positive contribution to m_h of about 35%. Since Point K had $m_h \sim 115 \text{ GeV}$, turning off c_6 and c_7 would make such a point excluded by LEP. However, larger radiative corrections than we have assumed could be present, thus compensating the contribution from c_6 and c_7 . A similar issue is present in most of the $\tan\beta = 20$ examples, but not in the $\tan\beta = 2$ ones.

We also note that we have assumed that $M = 1 \text{ TeV}$, while the current bounds on a W' with sequential SM

TABLE IX. Examples of UV completions that could lead to the set of effective operators of our benchmark points. The parameters λ_S , $\tilde{\lambda}_T$, λ_T and $\lambda_{\bar{T}}$ were defined in Eqs. (6) and (8), and may be complex. \tilde{g} and g' are the gauge couplings for a heavy W' and Z' , respectively, (see Ref. [6]).

Point	$\tan\beta$	λ_S^2	$\tilde{\lambda}_T^2$	λ_T	$\lambda_{\bar{T}}$	\tilde{g}^2	g'^2	Q_u	Q_d	c_6	c_7
F	2	0.17	-1.7	1.8	2.8	0	1.1	1/2	1/2	0.89	-0.08
A'	2	0.36	0.01	1.3	1.5	0.28	0.49	1/2	1/2	-0.38	-0.29
B'	2	-0.24	0.37	1.2	1.4	0	0.86	1/2	1/2	-0.31	0.47
C'	2	0.21	0.52	0.72	1.0	0	0.08	1/2	1/2	-0.34	0.42
J	20	0	-2	2.5	1.6	0	1.6	1/2	1/2	-0.35	-0.18
K	20	-0.34	2.1	-1.9	0.13	0.25	0.66	1/2	1/2	-0.59	0.66
L	20	0.29	2.0	1.8	0.4	0	0.88	1/2	1/2	0.61	-0.92
M	6	-0.36	-0.21	1.8	0.62	0	0.87	1/2	1/2	0	0

couplings are about 2.15 TeV from ATLAS [55] and 2.27 TeV from CMS [56]. Similarly, the current bound on a Z' with SM couplings is 1.83 TeV from ATLAS [57] and 1.94 TeV from CMS [58]. However, in our examples the new $SU(2)$ coupling \tilde{g} is fairly suppressed, and in some cases vanishes. Similarly, the bounds on Z' depend on its couplings to the first two generations of quarks, which are not constrained by our analysis. Therefore, we conclude that such UV completions, with gauge resonances at a TeV, are not necessarily inconsistent with present direct bounds.

APPENDIX B: COMPUTING SIGNIFICANCES

In this Appendix we record the procedure used in the main text to compute the required luminosities for exclusion and discovery. A clear summary of the statistical details and relevant approximations can be found in Appendix A of Ref. [36] (see also Refs. [59,60]).

As a first step, we compute, for each relevant channel/bin i , the following quantity

$$Q_i(\mathcal{L}_0) = \frac{R_i^{\text{mod}}}{R_i^{\text{exp}}(\mathcal{L}_0)}, \quad (\text{B1})$$

where R_i^{mod} is the rate (i.e., production cross section times branching fraction) for channel/bin i in a given model, and R_i^{exp} is the exclusion limit at the 95% CL on this rate, as reported by the experimental collaborations with a total integrated luminosity \mathcal{L}_0 . Sometimes the experimental limit is presented normalized to the SM, or to some other reference model, in which case R_i^{mod} should be normalized in the same way.

While R_i^{mod} does not change with luminosity, R_i^{exp} does. Under the hypothesis that the model in question is actually realized by nature, and in the Gaussian limit, the significance of a (downward) fluctuation by S_i , is given by $n_i = S_i/\sqrt{S_i + B_i}$ (neglecting systematic effects). Thus, in this limit, and assuming that the data reflects expected background only, we simply have

$$R_i^{\text{exp}}(\mathcal{L}) \approx \frac{R_i^{\text{exp}}(\mathcal{L}_0)}{\sqrt{\mathcal{L}/\mathcal{L}_0}}, \quad (\text{B2})$$

since both signal and background scale linearly with the total integrated luminosity. The exclusion is more stringent if a larger dataset is used, as expected.

Defining $R_i^{\text{exp}}(\mathcal{L}_0) = R_{i,0}$ and $Q_{i,0} = R_i^{\text{mod}}/R_{i,0}$ [$= Q_i(\mathcal{L}_0)$], one then has that

$$Q_i(\mathcal{L}) = \frac{R_i^{\text{mod}}}{R_{i,0}} \sqrt{\mathcal{L}/\mathcal{L}_0} = Q_{i,0} \sqrt{\mathcal{L}/\mathcal{L}_0}. \quad (\text{B3})$$

Since $Q_i(\mathcal{L}) = 1$ corresponds to exclusion at the 95% CL in channel/bin i , the future projection based on the above simple scaling indicates that the luminosity required to claim exclusion (of the given model) at the 95% CL is given by

$$\mathcal{L}_2 = \left(\frac{R_{i,0}}{R_i^{\text{mod}}}\right)^2 \mathcal{L}_0 = \left(\frac{1}{Q_{i,0}}\right)^2 \mathcal{L}_0. \quad (\text{B4})$$

One is also interested in estimating the discovery potential. Here one imagines that the (future) data shows a 5σ excess compared to the background-only expectation. In this case, the statistical significance under the background-only hypothesis, in the limit of a large number of events, is given by $n_i = S_i/\sqrt{B_i}$ (again neglecting systematics). If we use the current expectation for the background, scaled by $\sqrt{\mathcal{L}}$ to estimate the expected background with the higher luminosity, and assume also that $B_i \gg S_i$, we can relate the discovery potential to the quantities for exclusion defined above, since the measures for exclusion and discovery significance coincide in this limit. Thus, if the given model was indeed realized by nature, and the future data reflected the expected rate, one would be able to claim a discovery for a luminosity given by

$$\mathcal{L}_5 = \left(\frac{5}{2}\right)^2 \left(\frac{1}{Q_{i,0}}\right)^2 \mathcal{L}_0 = \frac{25}{4} \mathcal{L}_2. \quad (\text{B5})$$

Here we used that, under the above hypothesis, the current exclusion (based on data that reflect background only) would correspond to a 2σ downward fluctuation, and has $Q_{i,0} = 1$. In the absence of such a fluctuation, one would have had a “ 2σ hint” with current data.

Throughout this work we make use of Eqs. (B4) and (B5) to compute the required luminosity for an exclusion or discovery, respectively.

- [1] ATLAS collaboration, Report No. ATLAS-CONF-2011-135.
- [2] CMS collaboration, Report No. CMS-PAS-HIG-11-022.
- [3] A. Strumia, *Phys. Lett. B* **466**, 107 (1999); A. Brignole, J. A. Casas, J. R. Espinosa, and I. Navarro, *Nucl. Phys. B* **666**, 105 (2003); M. Dine, N. Seiberg, and S. Thomas, *Phys. Rev. D* **76**, 095004 (2007).
- [4] P. Batra and E. Pontón, *Phys. Rev. D* **79**, 035001 (2009); K. Blum, C. Delaunay, and Y. Hochberg, *Phys. Rev. D* **80**, 075004 (2009); J. A. Casas, J. R. Espinosa, and I. Hidalgo, *J. High Energy Phys.* **01** (2004) 008; S. Cassel, D. M. Ghilencea, and G. G. Ross, *Nucl. Phys. B* **825**, 203 (2010); S. Cassel and D. M. Ghilencea, [arXiv:1103.4793](https://arxiv.org/abs/1103.4793); K. Cheung, S. Y. Choi, and J. Song, *Phys. Lett. B* **677**, 54 (2009); M. Berg, J. Edsjo, P. Gondolo, E. Lundstrom, and S. Sjors, *J. Cosmol. Astropart. Phys.* **08** (2009) 035; N. Bernal and A. Goudelis, *J. Cosmol. Astropart. Phys.* **03** (2010) 007; N. Bernal, K. Blum, M. Losada, and Y. Nir, *J. High Energy Phys.* **08** (2009) 053; C. Grojean, G. Servant, and J. D. Wells, *Phys. Rev. D* **71**, 036001 (2005); D. Bodeker, L. Fromme, S. J. Huber, and M. Seniuch, *J. High Energy Phys.* **02** (2005) 026; C. Delaunay, C. Grojean, and J. D. Wells, *J. High Energy Phys.* **04** (2008) 029; K. Blum and Y. Nir, *Phys. Rev. D* **78**, 035005 (2008); K. Blum, C. Delaunay, M. Losada, Y. Nir, and S. Tulin, [arXiv:1003.2447](https://arxiv.org/abs/1003.2447); N. Bernal, M. Losada, and F. Mahmoudi, [arXiv:1104.5395](https://arxiv.org/abs/1104.5395); W. Altmannshofer, M. Carena, S. Gori, and A. de la Puente, [arXiv:1107.3814](https://arxiv.org/abs/1107.3814).
- [5] I. Antoniadis, E. Dudas, and D. M. Ghilencea, *J. High Energy Phys.* **03** (2008) 045; I. Antoniadis, E. Dudas, D. M. Ghilencea, and P. Tziveloglou, *Nucl. Phys. B* **808**, 155 (2009); AIP Conf. Proc. **1078**, 175 (2009); *Nucl. Phys. B* **831**, 133 (2010); *Nucl. Phys. B* **848**, 1 (2011).
- [6] M. Carena, K. Kong, E. Pontón, and J. Zurita, *Phys. Rev. D* **81**, 015001 (2010).
- [7] M. Carena, E. Pontón, and J. Zurita, *Phys. Rev. D* **82**, 055025 (2010); Proc. Sci., DIS2010 (2010) 212.
- [8] ATLAS collaboration, Report No. ATLAS-CONF-2011-134.
- [9] ATLAS Collaboration, *Phys. Rev. Lett.* **107**, 231801 (2011).
- [10] CMS collaboration, Report No. CMS-PAS-HIG-11-014.
- [11] G. Aad *et al.* (ATLAS Collaboration), *Phys. Lett. B* **705**, 435 (2011).
- [12] ATLAS Collaboration, *Phys. Rev. Lett.* **107**, 221802 (2011).
- [13] G. Aad *et al.* (ATLAS Collaboration), *Phys. Lett. B* **707**, 27 (2012).
- [14] CMS collaboration, Report Nos. CMS-PAS-HIG-11-013, CMS-PAS-HIG-11-015, CMS-PAS-HIG-11-016, and CMS-PAS-HIG-11-017.
- [15] ATLAS Collaboration, *Phys. Lett. B* **452**, 705 (2011).
- [16] CMS collaboration, Report No. CMS-PAS-HIG-11-021.
- [17] ATLAS collaboration, Report No. ATLAS-CONF-2011-132.
- [18] CMS collaboration, Report No. CMS-PAS-HIG-11-020.
- [19] CMS collaboration, Report No. CMS-PAS-HIG-11-012.
- [20] CMS collaboration, Report No. CMS-PAS-HIG-11-008.
- [21] M. Carena, P. Draper, T. Liu, and C. Wagner, *Phys. Rev. D* **84**, 095010 (2011).
- [22] U. Ellwanger, G. Espitalier-Noel, and C. Hugonie, [arXiv:1107.2472](https://arxiv.org/abs/1107.2472).
- [23] S. Chang, J. A. Evans, and M. A. Luty, *Phys. Rev. D* **84**, 095030 (2011).
- [24] E. Weihs and J. Zurita, [arXiv:1110.5909](https://arxiv.org/abs/1110.5909).
- [25] T. Aaltonen *et al.* (CDF and D0 Collaboration), *Phys. Rev. D* **82**, 011102 (2010).
- [26] T. Aaltonen *et al.* (CDF and D0 Collaborations), *Phys. Rev. Lett.* **104**, 061802 (2010).
- [27] CMS collaboration, Report No. CMS NOTE 2010/008.
- [28] ATLAS collaboration, Report No. ATL-PHYS-PUB-2010-015.
- [29] http://www-cdf.fnal.gov/physics/new/hdg/Results_files/results/hgamgam_apr11/10485_HiggsGamGam7Public.pdf.
- [30] <http://www-d0.fnal.gov/Run2Physics/WWW/results/prelim/HIGGS/H103/H103.pdf>.
- [31] P. Bechtle, O. Brein, S. Heinemeyer, G. Weiglein, and K. E. Williams, *Comput. Phys. Commun.* **181**, 138 (2010); [arXiv:0811.4169](https://arxiv.org/abs/0811.4169); [arXiv:0905.2190](https://arxiv.org/abs/0905.2190), in *SUSY09: 7th International Conference on Supersymmetry and the Unification of Fundamental Interactions*, edited by G. Alvenson, P. Nath, and B. Nelson, AIP Conf. Proc. No. 1200, (AIP, New York, 2010), p. 510. [arXiv:0909.4664](https://arxiv.org/abs/0909.4664) [arXiv:1012.5170](https://arxiv.org/abs/1012.5170)
- [32] P. Bechtle, O. Brein, S. Heinemeyer, G. Weiglein, and K. E. Williams, *Comput. Phys. Commun.* **182**, 2605 (2011).
- [33] ATLAS collaboration, Report No. ATLAS-CONF-2011-103.
- [34] J. M. Butterworth, A. R. Davison, M. Rubin, and G. P. Salam, *Phys. Rev. Lett.* **100**, 242001 (2008).
- [35] P. Draper, T. Liu, and C. E. M. Wagner, *Phys. Rev. D* **80**, 035025 (2009).
- [36] P. Draper, T. Liu, and C. E. M. Wagner, *Phys. Rev. D* **81**, 015014 (2010).
- [37] D. Benjamin *et al.* (Tevatron New Phenomena & Higgs Working Group), [arXiv:1003.3363](https://arxiv.org/abs/1003.3363).
- [38] S. Dittmaier, C. Mariotti, G. Passarino, R. Tanaka *et al.* (LHC Higgs Cross Section Working Group), Handbook of LHC Higgs Cross Sections: 1. Inclusive Observables, [arXiv:1101.0593v3](https://arxiv.org/abs/1101.0593v3).
- [39] R. V. Harlander and W. B. Kilgore, *Phys. Rev. D* **68**, 013001 (2003).
- [40] A. D. Martin, W. J. Stirling, R. S. Thorne, and G. Watt, *Eur. Phys. J. C* **63**, 189 (2009).
- [41] J. F. Gunion, H. E. Haber, G. L. Kane, and S. Dawson, *Front. Phys.* **80**, 1 (2000).
- [42] M. Jezabek and J. H. Kuhn, *Nucl. Phys. B* **314**, 1 (1989).
- [43] C. S. Li and T. C. Yuan, *Phys. Rev. D* **42**, 3088 (1990); **47**, 2156 (1993); **47**, 2156 (1993).
- [44] A. Czarnecki and S. Davidson, *Phys. Rev. D* **48**, 4183 (1993).
- [45] M. S. Carena, D. Garcia, U. Nierste, and C. E. M. Wagner, *Nucl. Phys. B* **577**, 88 (2000).
- [46] L. J. Hall, R. Rattazzi, and U. Sarid, *Phys. Rev. D* **50**, 7048 (1994); M. S. Carena, M. Olechowski, S. Pokorski, and C. E. M. Wagner, *Nucl. Phys. B* **426**, 269 (1994); D. M. Pierce, J. A. Bagger, K. T. Matchev, and R. j. Zhang, *Nucl. Phys. B* **491**, 3 (1997).
- [47] ATLAS collaboration, Report No. ATLAS-CONF-2011-130.

- [48] ATLAS collaboration, Report No. ATLAS-CONF-2011-098.
- [49] V.M. Abazov *et al.* (D0 Collaboration), *Phys. Lett. B* **693**, 95 (2010).
- [50] S. Chatrchyan *et al.* (CMS Collaboration), Report Nos. CMS-SUS-10-009 and CERN-PH-EP-2011-099; ATLAS collaboration, Report Nos. ATLAS-CONF-2011-086, ATLAS collaboration and ATLAS-CONF-2011-090.
- [51] G.G. Ross and K. Schmidt-Hoberg, [arXiv:1108.1284](#).
- [52] H.M. Lee, S. Raby, M. Ratz, G.G. Ross, R. Schieren, K. Schmidt-Hoberg, and P.K.S. Vaudrevange, *Nucl. Phys.* **B850**, 1 (2011).
- [53] A. Delgado, C. Kolda, J.P. Olson, and A. de la Puente, *Phys. Rev. Lett.* **105**, 091802 (2010); *Phys. Rev. D* **82**, 035006 (2010); J. de Blas and A. Delgado, *Phys. Rev. D* **83**, 115011 (2011); [arXiv:1108.2511](#).
- [54] K. Agashe, A. Azatov, A. Katz, and D. Kim, [arXiv:1109.2842](#) [*Phys. Rev. D* (to be published)].
- [55] G. Aad *et al.* (ATLAS Collaboration), *Phys. Lett. B* **705**, 28 (2011).
- [56] CMS collaboration, Report No. CMS-PAS-EXO-11-024.
- [57] Atlas Collaboration, *Phys. Rev. Lett.* **107**, 272002 (2011).
- [58] CMS collaboration, Report No. CMS-PAS-EXO-11-019.
- [59] G. Aad *et al.* (The ATLAS Collaboration), [arXiv:0901.0512](#).
- [60] G.L. Bayatian *et al.* (CMS Collaboration), *J. Phys. G* **34**, 995 (2007).